

**Optimization of the metabolic stability of a fluorinated cannabinoid receptor
subtype 2 (CB₂) ligand designed for PET studies**

Dominik Heimann,^{a,§} Frederik Börgel,^{a,§} Henk de Vries,^b Marius Patberg,^a Eliot Jan-Smith,^a Bastian Frehland,^a Dirk Schepmann,^a Laura H. Heitman,^b Bernhard Wunsch^{a,c}

§ Both authors contributed equally to this work.

^a Institut für Pharmazeutische und Medizinische Chemie der Universität Münster, Corrensstraße 48, D-48149 Münster, Germany.

Tel.: +49-251-8333311; Fax: +49-251-8332144; E-mail: wuensch@uni-muenster.de

^b Division of Medicinal Chemistry, Leiden Academic Centre for Drug Research, Leiden University, P.O. Box 9502, 2300 RA Leiden, The Netherlands.

^c Cells-in-Motion Cluster of Excellence (EXC 1003 – CiM), Westfälische Wilhelms-Universität Münster, Germany.

Abstract

The central CB₂ receptor represents a promising target for the treatment of neuroinflammatory diseases as CB₂ activation mediates anti-inflammatory effects. Recently, the 18-F labeled PET radiotracer [¹⁸F]**7a** was reported, which shows high CB₂ affinity and high selectivity over the CB₁ subtype but low metabolic stability due to hydrolysis of the amide group. Based on these findings twelve bioisosteres of **7a** were synthesized containing a non-hydrolysable functional group instead of the amide group. The secondary amine **23a** ($K_i = 7.9$ nM) and the ketone **26a** ($K_i = 8.6$ nM) displayed high CB₂ affinity and CB₂:CB₁ selectivity in *in vitro* radioligand binding studies. Incubation of **7a**, **23a** and **26a** with mouse liver

microsomes and LC-quadrupole-MS analysis revealed a slightly higher metabolic stability of secondary amine **23a**, but a remarkably higher stability of ketone **26a** in comparison to amide **7a**. Furthermore, a $\log D_{7.4}$ value of 5.56 ± 0.08 was determined for ketone **26a** by micro shake-flask method and LC-MS quantification.

Key words

CB₂ receptor ligands, Amide bioisosteres, Fluorinated carbazole derivatives, Structure affinity relationships, Metabolic stabilization, Identification of metabolites, PET

1. Introduction

The relaxing and euphoric properties of *Cannabis sativa* have led to a worldwide use as therapeutic and intoxicant. In 1964 one of the responsible psychoactive compounds, Δ^9 -tetrahydrocannabinol (THC), was isolated and characterized for the first time [1]. With these findings it was possible to unravel the endogenous cannabinoid (endocannabinoid) system in the following decades. Today it is known that it is a complex lipid signaling network, which comprises the arachidonic acid-derived ligands N-arachidonylethanolamide (anandamide, AEA) [2] and 2-arachidonoylglycerol (2-AG) [3], the two classical cannabinoid receptors (CB₁ and CB₂) [4],[5] and the enzymes responsible for the biosynthesis (e.g. *N*-acyltransferase, diacylglycerol lipase) and inactivation (e.g. fatty acid amide hydrolases, monoacylglycerol lipases) of the natural ligands. The affiliation of further ligands (e.g. 2-arachidonoylglycerol ether, *N*-arachidonoyldopamine, hemopressin) and other receptors (e.g. transient receptor potential vanilloid type 1) is still discussed [6],[7].

The two classical cannabinoid receptors (CB₁ and CB₂) belong to the class of G_{i/o} protein coupled receptors and show a 44 % sequence homology [8]. They differ

mainly in their expression pattern. Due to an increased expression in peripheral tissues (e.g. immune cells; reproductive, cardiovascular, gastrointestinal and respiratory system) the CB₂ receptor was designated as the peripheral receptor [9]. Compared to the CB₁ receptor, which is mainly expressed in the brain, the CB₂ receptor expression in the central nervous system (CNS) is rather low [8],[10]. However, the presence of CB₂ receptors could be shown in microglia, human cerebral microvascular endothelial cells and human fetal astrocytes [9],[10],[11]. Especially under neuroinflammatory conditions the receptor is overexpressed [12] and activation by an agonist leads to anti-inflammatory effects [9]. Therefore, the receptor is an interesting target for neurodegenerative and neuroinflammatory disorders like Alzheimer's disease, Huntington's disease, multiple sclerosis, depression and schizophrenia [9].

In order to examine expression sites and the neurophysiological function of the CB₂ receptor, adequate tools are required. Besides CB₂ receptor knockout mice [13], several agonists (e.g. JWH 133) [14], antagonists (e.g. SR144528 and AM630) [15],[16] and partly unselective antibodies [17] are currently used in research. Another possibility to investigate the CB₂ receptor expression and distribution is the use of positron emission tomography (PET) tracers. This approach is a non-invasive method that can be used to quantitatively visualize expression patterns of the receptor under healthy and pathological conditions, to monitor the progress of a neuroinflammation, and to determine pharmacokinetic (e.g. uptake into the CNS, reversibility of target binding and wash-out) and pharmacodynamic properties of new therapeutics [18]. So far, appropriate ¹¹C or ¹⁸F labeled tracers don't exist possessing high CB₂ affinity and sufficient selectivity over other targets, suitable physicochemical (e.g. moderate lipophilicity) and pharmacokinetic properties (e.g. good penetration into the CNS, the absence of radiolabeled metabolites). In recent years, numerous

attempts have been made to address this problem.

Trisubstituted pyridine derivative [^{11}C]RSR-056 (**1**) reveals high CB_2 affinity ($K_i = 2.5$ nM) and has an experimentally determined optimal $\log D_{7.4}$ value of 1.94 for a CNS PET tracer. However, the metabolic stability in male Wistar rats is rather low [19]. The thiophene based PET tracer [^{11}C]AAT-015 (**2**) is washed out rapidly from mouse/rat spleen tissue. A specific binding to the CB_2 receptor couldn't be shown in PET studies [20]. Moreover, both PET tracers **1** and **2** contain ^{11}C radioisotopes with a short half-life of 20 min, limiting broad application in clinics without cyclotron nearby. Radiotracers containing fluorine-18 with a half-life of 110 minutes are therefore preferred. 4-Oxoquinoline derivative [^{18}F]RS-126 (**3**) contains ^{18}F but shows rapid *in vivo* metabolic defluorination. Penetration of the intact tracer into the brain could therefore not be confirmed [21]. Brain penetrating radiometabolites were also shown for [^{18}F]29 (**4**), which makes the interpretation of the images difficult. In addition, the radiofluorination to obtain **4** has proven to be quite challenging. Radiochemical yields did not exceed 16 ± 8.7 %, when an automated module was used [22]. Similar problems occurred during the radiosynthesis of a PET tracer with $\text{OCD}_2^{18}\text{F}$ moiety described by Hortala et al. Due to a three-step radiosynthesis, the overall radiochemical yield was low (0.3 – 1.6 %) [23]. The radiofluorination to yield [^{18}F]CB91 (**5**) also caused problems as an unexpected non-radioactive peak appeared in the HPLC chromatogram [24]. In 2016 the quinolineamine [^{18}F]MA3 (**6**) was reported, displaying high CB_2 affinity and selectivity over the human CB_1 receptor, but a rapid wash-out from brain (Figure 1) [25].

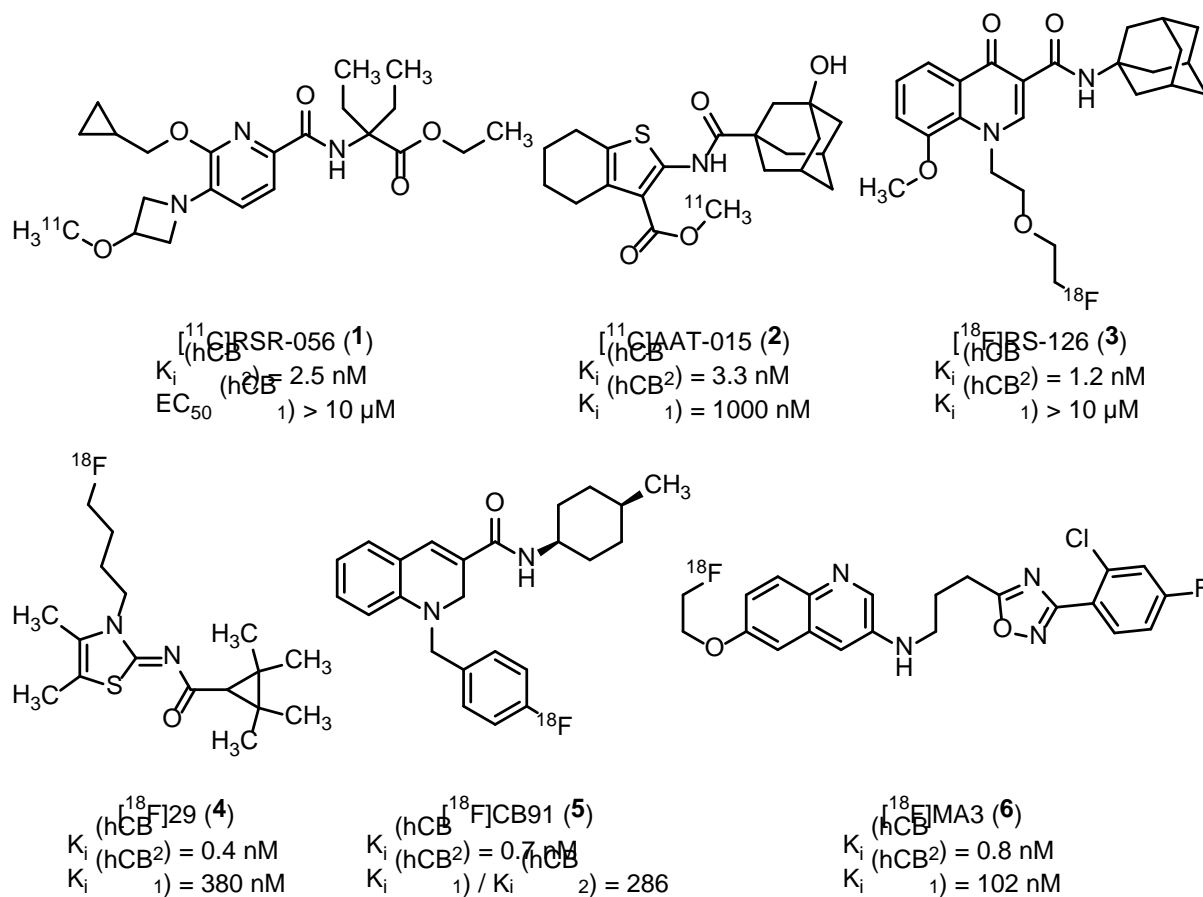


Figure 1. Potential CB₂ receptor radioligands for PET imaging.

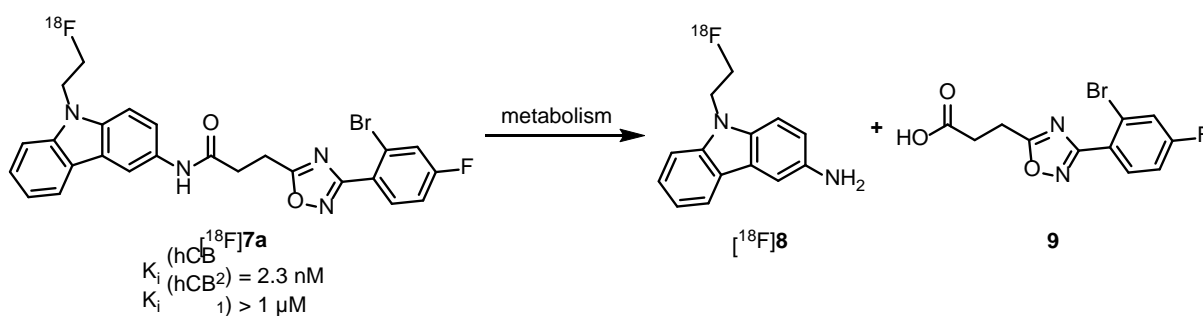
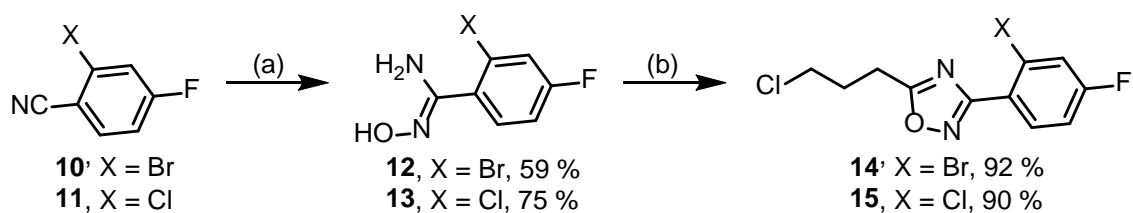


Figure 2. Metabolism of [¹⁸F]7a.

Very recently, we reported the synthesis, radiosynthesis and biological evaluation of the CB₂ receptor radiotracer [¹⁸F]7a containing a comparable aryl-oxadiazolyl-alkyl moiety as [¹⁸F]MA3 (6) [26],[27]. In addition to high CB₂ affinity and selectivity over

the CB₁ receptor, the penetration into the mouse brain and low defluorination tendency *in vivo* could be demonstrated. In further studies the high lipophilicity of **7a** (logD = 3.82 – 4.21) [26] should be reduced, which can contribute to a high non-specific binding. Furthermore, fast metabolic hydrolysis of the amide to the corresponding amine [¹⁸F]**8** and carboxylic acid **9** was observed during *in vivo* experiments with mice (Figure 2). In this work, we aim to synthesize metabolically more stable fluorinated CB₂ receptor ligands by replacing the hydrolysis-sensitive amide group by functional groups, which can't be hydrolyzed. CB₂ and CB₁ receptor affinity will determine the selection of a new generation of CB₂-PET-tracer.

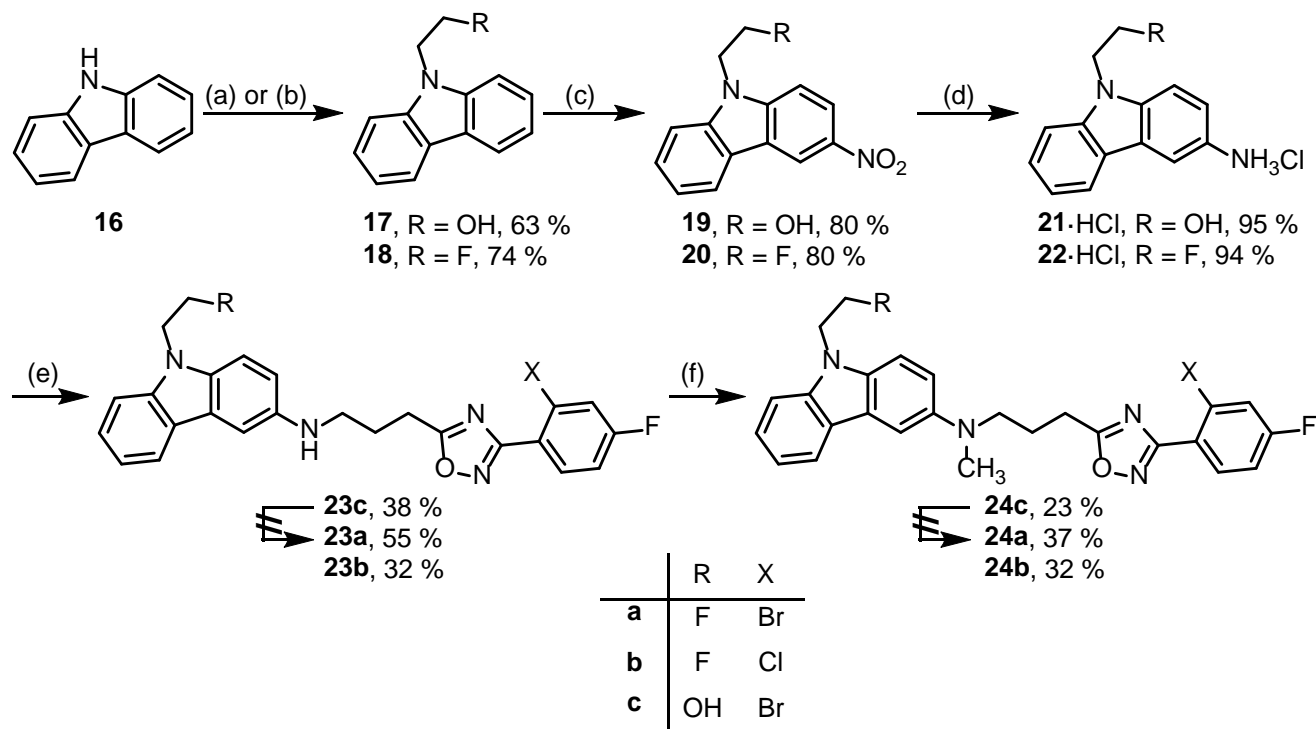
2. Synthesis



Scheme 1. Reagents and reaction conditions: (a) H₂NOH·HCl, Na₂CO₃, H₂O, MeOH/EtOH, rt → reflux. (b) 4-chlorobutyl chloride, EtN*i*Pr₂, toluene, 0 °C → rt → reflux.

In a first approach, the amide of **7a** was replaced by secondary and tertiary amines. In addition to the bromine atom described by Rühl et al. in 2-position of the phenyl moiety, compounds with a chlorine atom in 2-position described by Cheng et al. (see also **6**) were synthesized in order to reduce the molecular mass and to slightly increase the polarity [28],[29]. For the preparation of **23a-c** and **24a-c** a convergent synthesis was designed. For this purpose, nitriles **10** and **11** were treated with an excess of hydroxylamine hydrochloride under basic conditions [26],[30]. Whilst 1.3

equivalents of hydroxylamine hydrochloride led to a yield of 75 % of **13**, an increase to 3 equivalents and reduction of the temperature decreased the yield to 59 % of **12** due to an increased formation of by-products. Treatment of the resulting benzamidoximes **12** and **13** with 4-chlorobutyryl chloride and ethyldiisopropylamine afforded the alkyl halides **14** and **15**, respectively (Scheme 1).



Scheme 2. Reagents and reaction conditions: (a) 1. *n*-BuLi, ethylene sulfate, THF, $-78\text{ }^{\circ}\text{C} \rightarrow \text{rt}$; 2. H_2SO_4 97 %, water, reflux. (b) NaH, DMF, $\text{TsOCH}_2\text{CH}_2\text{F}$, $0\text{ }^{\circ}\text{C} \rightarrow \text{rt}$. (c) HNO_3 65 %, CH_2Cl_2 , $0\text{ }^{\circ}\text{C}$. (d) 1. H_2 , Pd/C 10 %, THF, 1 bar, rt; 2. HCl in Et_2O . (e) **14** or **15**, NEt_3 , Bu_4NI , toluene, reflux. (f) CH_3I , NEt_3 , CH_3CN , reflux.

The second building block **21**·HCl was prepared according to literature [31]. Carbazole **16** was deprotonated with *n*-butyllithium and subsequently treated with ethylene sulfate to yield the hydroxyalkylated carbazole **17**, which was nitrated with nitric acid at $0\text{ }^{\circ}\text{C}$. Hydrogenation catalyzed by Pd/C provided the primary aromatic amine **21**, which was precipitated as hydrochloride salt **21**·HCl (Scheme 2). Coupling

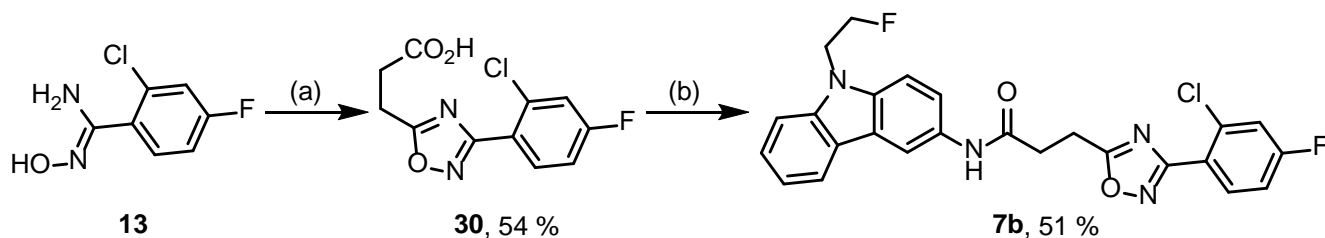
of **21**·HCl with **14** was performed with triethylamine and tetrabutylammonium iodide in toluene. Common polar aprotic solvents like acetonitrile, *N,N*-dimethylformamide and pyridine led to increased formation of polar side products. The secondary amine **23c** was further methylated with iodomethane in the presence of triethylamine to provide the tertiary amine **24c** in 23 % yield (Scheme 2).

Different deoxofluorination reagents (DAST, XtalFluor-E[®] and Fluolead[™]) were investigated for the conversion of the alcohols **23c** and **24c** to the corresponding fluoroalkanes **23a** and **24a**. However, all attempts failed to give the fluoroalkanes **23a** and **24a**. It is assumed that the amine-moiety is responsible for side reactions. Hence, it was decided to introduce the fluorine atom at an earlier stage into the compounds. Therefore, fluoroethyl tosylate in the presence of sodium hydride was used for the fluoroalkylation of carbazole in the first step of the synthesis, leading to 74 % yield of carbazole **18** [32],[33]. As described for the alcohol **17**, the fluoro derivative was nitrated with nitric acid and subsequently reduced with hydrogen and Pd/C to afford the carbazolamine hydrochloride **22**·HCl in 75 % yield over two steps. Alkylation of **22**·HCl with chloroalkanes **14** and **15** led to the secondary amines **23a-b**, which were transformed into tertiary amines **24a-b** upon treatment with iodomethane (Scheme 2).

In a second approach, the amide of **7a** was replaced bioisosterically by a ketone **26a**. Therefore, fluoroethylcarbazole **18** was reacted with 4-(methoxycarbonyl)butanoyl chloride and BF₃·Et₂O in a Friedel-Crafts acylation. Usage of aluminum chloride as Lewis acid resulted in a halogen exchange of the fluorine atom with a chloride atom, as described in the literature [34]. Therefore, a fluoride-containing Lewis acid was used. The obtained ester was directly hydrolyzed with sodium hydroxide to the carboxylic acid **25**. In this case glutaric anhydride as acylation reagent in combination with Lewis acids had turned out to be too unreactive. After activation with COMU[®], **25**

26a to alcohol **28a** was performed with NaBH₄ in a mixture of methanol and ethyl acetate. Since the conversion of ketone **26a** was incomplete due to its poor solubility, **26b** was reacted with the more reactive lithium borohydride in THF, which resulted in a higher yield of 63 %.

In order to better understand replacement of the amide by bioisosteric functional groups, the parent amide **7b** with a chlorine atom in 2-position had to be prepared. For this purpose, amidoxime **13** was reacted with succinic anhydride as described in literature [29] and the resulting carboxylic acid **30** was coupled with **22**·HCl in the presence of COMU[®] (Scheme 4).



Scheme 4. Reagents and reaction conditions: (a) succinic anhydride, DMF, 120 °C. (b) COMU[®], EtNⁱPr₂, carbazolamine hydrochloride **22**·HCl, THF, rt → 0 °C → rt.

3. Receptor affinity

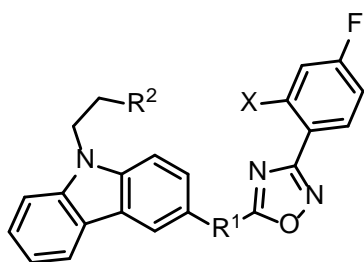


Table 1. CB₁ and CB₂ binding affinity of test compounds.

compd	R ¹	R ²	X	K _i (hCB ₂) ± SEM [nM] ^a	displacement (hCB ₁) ^b
7a		F	Br	2.9 ± 0.4	22 % ^c
7b		F	Cl	1.5 ± 0.1	10 %
23a		F	Br	7.9 ± 1.4	- 10 %
23b		F	Cl	7.1 ± 1.2	10 %
23c		OH	Br	99 ± 22	9 %
24a		F	Br	128 ± 12	- 10 %
24b		F	Cl	110 ± 8.3	- 10 %
24c		OH	Br	55 %	12 %
26a		F	Br	8.6 ± 2.4	59 %
26b		F	Cl	11 ± 1.8	44 %
27a		F	Br	13 ± 0.5	28 %
27b		F	Cl	15 ± 1.7	37 %
28a		F	Br	20 ± 2.7	9 %
28b		F	Cl	n.d. ^d	n.d. ^d
29a		F	Br	56 %	5 %
29b		F	Cl	n.d. ^d	n.d. ^d

CP 55,940	8.44 ± 0.2	9.26 ± 0.1
WIN 55,212-2	8.57 ± 0.2	8.72 ± 0.2
HU 210	9.78 ± 0.04	9.55 ± 0.06

^aThe reported K_i -values are mean values of three independent experiments ($n = 3$).

^bDue to the low hCB₁ affinity, only the radioligand displacement at a test compound concentration of 1 μM is given. Mean value of two independent experiments ($n = 2$).

^cMean value of four experiments ($n = 4$). ^dn.d. = not determined due to low stability.

The CB₁ and CB₂ receptor affinity was determined in competition binding experiments with the radioligand [³H]CP-55,940 and fragments of CHO-K1 cells expressing the CB₁ or CB₂ receptor. Rimonabant (SR141716A) and AM630 were used for the identification of the non-specific binding of the radioligand, towards CB₁ and CB₂ receptors, respectively.

As shown in Table 1, amide **7b** with a 2-chloro-4-fluorophenyl substituent represents a ligand with a high CB₂ affinity ($K_i = 1.5$ nM) and selectivity over the CB₂ receptor (> 500), which is comparable to lead compound **7a** ($K_i = 2.9$ nM). These results correlate with the affinity data of the CB₂ receptor PET tracer [¹⁸F]MA3 (**6**), which has the same phenyl substitution pattern [25].

Replacement of the NH-C=O-moiety by two methylene groups slightly decreased CB₂ receptor affinity as reflected by K_i values of 13 nM and 15 nM for alkanes **27a** and **27b**. This result indicates that the amide group increases CB₂ affinity but is not essential for binding at the CB₂ receptor. Moreover, the replacement of the amide group by an ethylene group led to increased lipophilicity. This effect could contribute to the high CB₂ affinity, since in principle lipophilic compounds preferentially bind to the cannabinoid receptors.

The secondary and tertiary amines **23a,b** and **24a,b**, with a methylene moiety instead

of the carbonyl moiety of the amides **7a,b**, show an increased hydrophilicity in comparison to the alkanes **27a** and **27b**. Secondary amines **23a** and **23b** possess additional H-bond donor and acceptor groups compared to the alkanes and display high CB₂ receptor affinity with K_i values of 7.9 nM and 7.1 nM, respectively. This is consistent with the published data of CB₂ receptor PET-tracer [¹⁸F]MA3 (**6**, K_i = 0.8 nM) with arylamine substructure [25]. Replacement of the aliphatic fluorine atom by a polar hydroxy group (**23c**) led to 13-fold decreased CB₂ affinity (K_i = 99 nM). Also, the conversion of the secondary amines **23a,b** into tertiary methylamines **24a,b** resulted in a 16-fold loss of CB₂ affinity. The significantly reduced CB₂ affinity of alcohol **24c** confirms that the polar hydroxyethyl moiety is not tolerated by the CB₂ receptor.

The secondary alcohol **28a** possesses similar pharmacological properties as the secondary amine **23a**. With a K_i (hCB₂) of 20 nM, **28a** is a selective CB₂ receptor ligand that has slightly lower CB₂ affinity than the amide **7a**.

Ketones **26a** and **26b** exhibit an electron withdrawing effect on the carbazole system and mimic, due to the sp²-hybridized carbonyl moiety, the planar structure of the amide group of **7a,b**. With K_i (hCB₂) values of 8.6 nM and 11 nM, the ketones **26a** and **26b** reveal high CB₂ affinity, respectively, and about 100-fold selectivity over the CB₁ subtype. In contrast, a much lower affinity was recorded for oxime **29a**. At a test compound concentration of 1 μM, only 56 % of the radioligand was displaced, suggesting a K_i (hCB₂) value in this concentration range. It is possible that the low affinity of oxime **29a** is due to low stability as observed for the analog **29b**.

Compounds with a 2-chloro-4-fluoro substitution pattern of the terminal phenyl ring show comparable CB₂ affinity as the corresponding 2-bromo-4-fluoro substituted derivatives. With exception of the moderate affine tertiary amines **24**, the K_i values differ only by 0.8 - 2.4 nM. In the case of the tertiary amines **24** a difference of 18 nM

was observed, which is due to the moderate CB₂ affinity in the 120 nM range. In relative terms, the *K_i* values of the amide bioisosteres differ only by 10 - 22%.

4. Metabolism studies of **7a**, **23a** and **26a**

In vivo studies with mice of [¹⁸F]**7a** showed low metabolic stability. Radiochromatograms of murine brain samples at 60 min after injection of [¹⁸F]**7a** revealed only 35 % of intact radiotracer [¹⁸F]**7a** [26]. Therefore, the metabolic stability of secondary amine **23a** and ketone **26a** was determined *in vitro* and compared to the *in vitro* metabolic stability of amide **7a**. The structures of the main metabolites were analyzed in order to identify metabolically labile structural elements and prove whether the bioisosteric replacement of the amide inhibits cleavage at the original amide position in the side chain. Compounds **23a** and **26a** were selected due to their high CB₂ affinity and selectivity and the same substitution pattern at the phenyl moiety as the lead compound **7a**.

4.1 Stability over time

For the *in vitro* stability studies, mouse liver microsomes were used with and without addition of the cofactor NADPH. After incubation of the test compounds (75 μM) for 90 min at 37 °C, the samples were analyzed by LC-quadrupole-MS. The amount of intact parent compound (in %) was calculated via external calibration in combination with an internal standard (ISTD).

Table 2. *In vitro* metabolic stability of potent CB₂ ligands **7a**, **23a** and **26a**.

compd.	amount of intact parent [%] (90 min, without NADPH, n = 4)	amount of intact parent ± SEM [%] (90 min, with NADPH, n = 4)
7a	73.3 ± 1.5	69.8 ± 0.5
23a	84.9 ± 1.7	75.1 ± 2.9 ^a
26a	99.1 ± 0.4	98.2 ± 0.6 ^b

One-Way ANOVA, post hoc mean comparison Tukey Test compared to **7a**,
^a p > 0.05. ^b p < 0.05.

The data in Table 2 indicate that an exchange of the amide moiety (NHC(=O)) of **7a** by an aminomethylene (NHCH₂) moiety (**23a**) only slightly increased the metabolic stability upon incubation with mouse liver microsomes and NADPH. However, ketone **26a** was not metabolically degraded, as 98.2 % of the parent ketone **26a** were still intact after an incubation period of 90 min. Ketone **26a** showed a significantly higher metabolic stability compared to secondary amine **23a** and amide **7a** (p < 0.05).

In a second experiment it was shown that degradation of amide **7a** and amine **23a** took place even in the absence of NADPH. Possible explanations for this observation are a low residual concentration of naturally occurring NADPH in the microsomal preparation or, alternatively, a NADPH independent metabolism, by e.g. microsomal amidases. Therefore, compounds **7a**, **23a** and **26a** were also incubated in murine blood serum for the identification of metabolites.

4.2 Identification of metabolite structures

For further investigation of the metabolism, incubated samples were analyzed using LC-qToF-MS, which allowed the identification of metabolites through exact masses and fragmentation experiments. To further analyze the stability, compounds **7a**, **23a**

and **26a** (75 μ M) were also incubated in mouse blood serum.

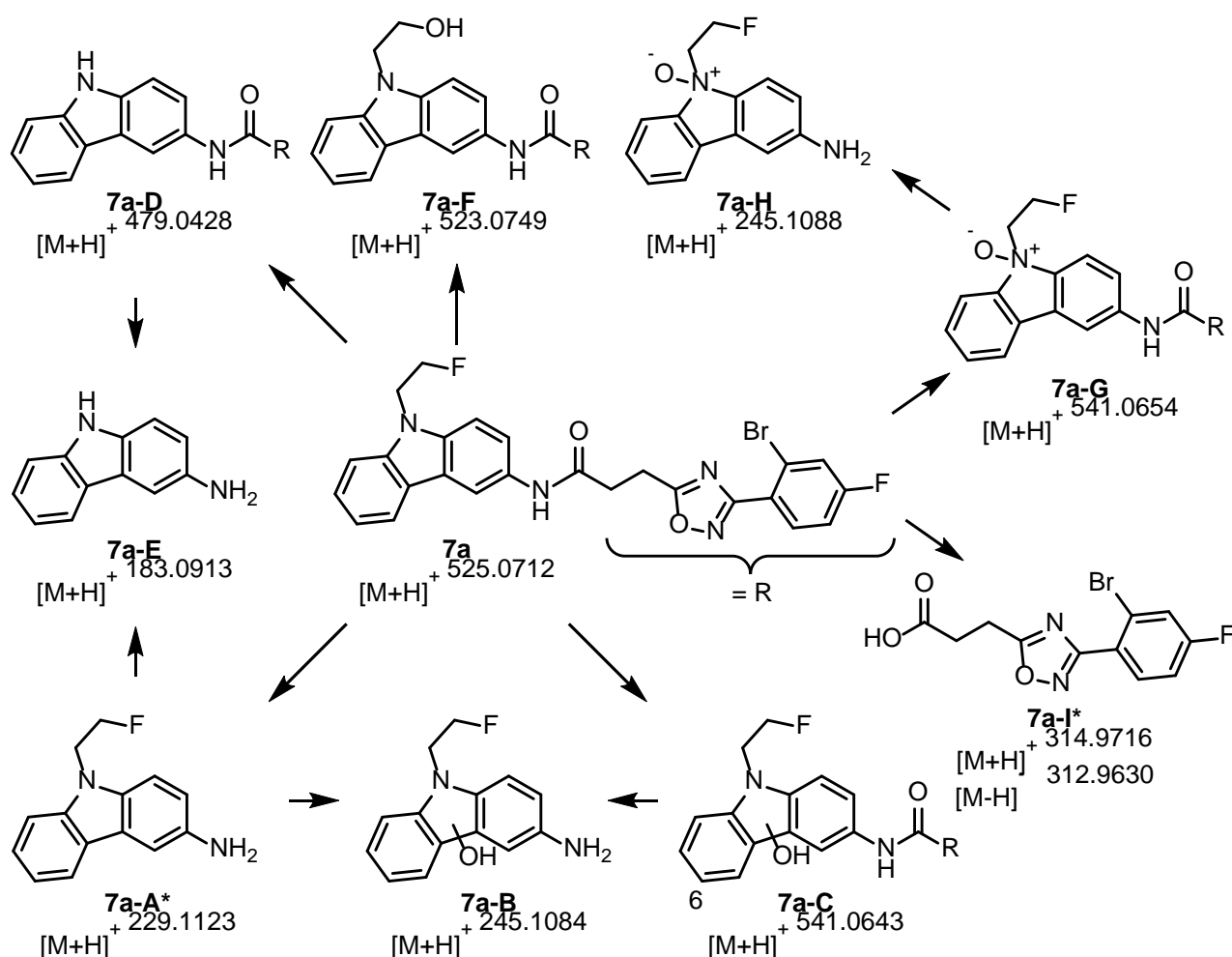


Figure 3. Proposed structures of metabolites identified 90 min after incubation of **7a** with mouse liver microsomes and NADPH. * The marked metabolites were also formed without NADPH.

In Figure 3 the metabolites formed after incubation of amide **7a** with rat liver microsomes and NADPH are displayed. Metabolite **7a-F** was obtained by defluorination. Although this metabolite was formed in minor amounts, the F-atom of the potential positron emitter is lost. The oxidative *N*-dealkylation resulted in carbazole **7a-D**, which was subsequently hydrolyzed to form the primary amine **7a-E**. This metabolite can also be formed by hydrolysis of the parent compound **7a** followed

by *N*-dealkylation of **7a-A**. Again, the F-atom bearing the radioactivity is lost in metabolites **7a-D** and **7a-E**. Although the position of the hydroxy group in the carbazole moiety of metabolite **7a-C** could not be assigned unequivocally, the 6-position is most likely bearing the OH moiety. Another primary aromatic amine **7a-B** resulted from amide hydrolysis. The structure of the *N*-oxide **7a-G** was confirmed by fragmentation analysis (Figure 4).

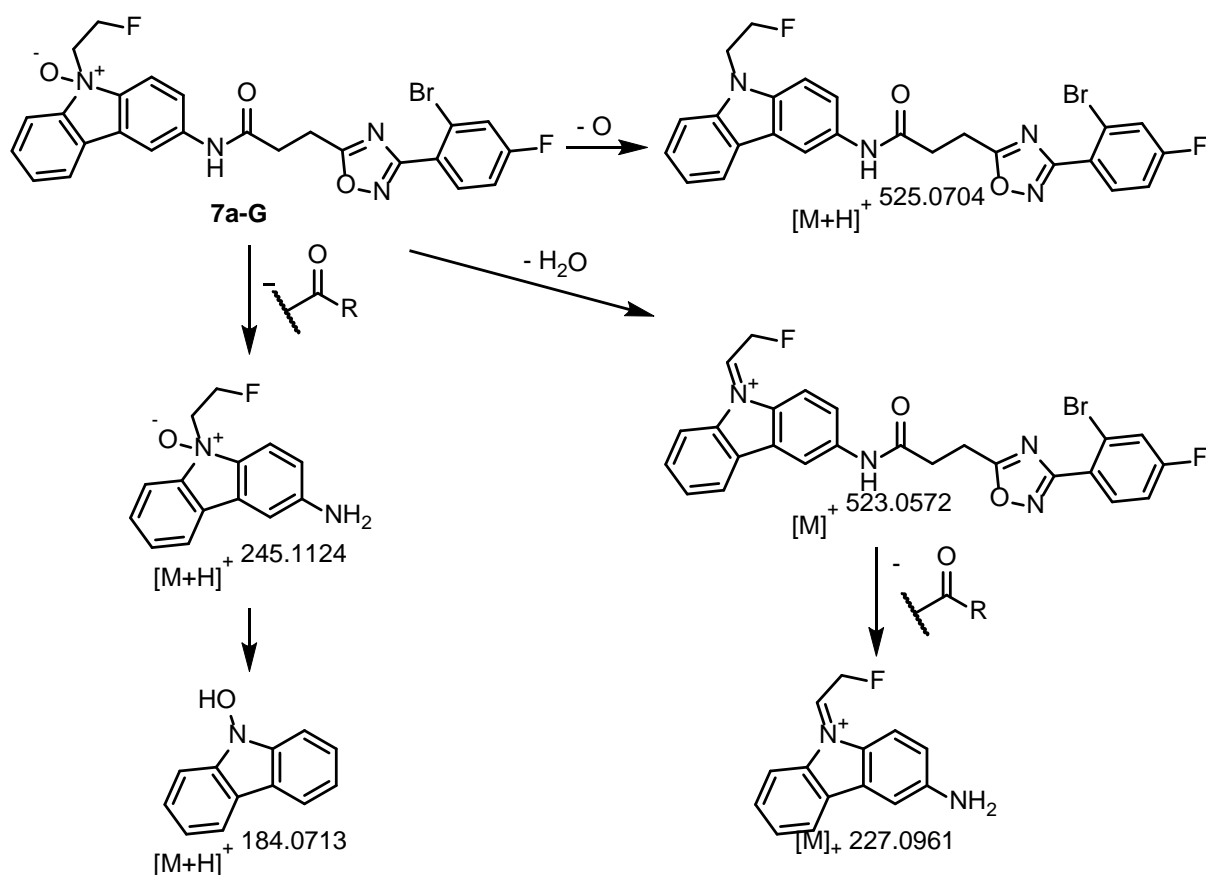


Figure 4. Fragmentation of *N*-oxide **7a-G**.

Since fragmentation of *N*-oxide **7a-G** led to a fragment (m/z 523.0572) formed by the loss of water, an aromatic hydroxylation was excluded. However, the loss of oxygen provided the fragment m/z 525.0704 (parent **7a**), which was reported for *N*-oxides [35]. Furthermore, the fragment m/z 184.0713 proves the additional O-atom of **7a-G** somewhere at the carbazole moiety.

Incubation of amide **7a** with mouse liver microsomes in presence and absence of NADPH led to hydrolysis of the amide moiety resulting in the primary aromatic amine **7a-A** ($[M+H]^+$ 229.1123) and the carboxylic acid **7a-I** ($[M+H]^+$ 314.9716, $[M-H]^-$ 312.9630). This hydrolysis is most likely caused by hydrolases (amidases) in the microsomes and was also observed during incubation with mouse blood serum. For similar compounds the hydrolysis of the amide was reported as major clearance pathway in *in vivo* experiments with mice and rats [26],[29].

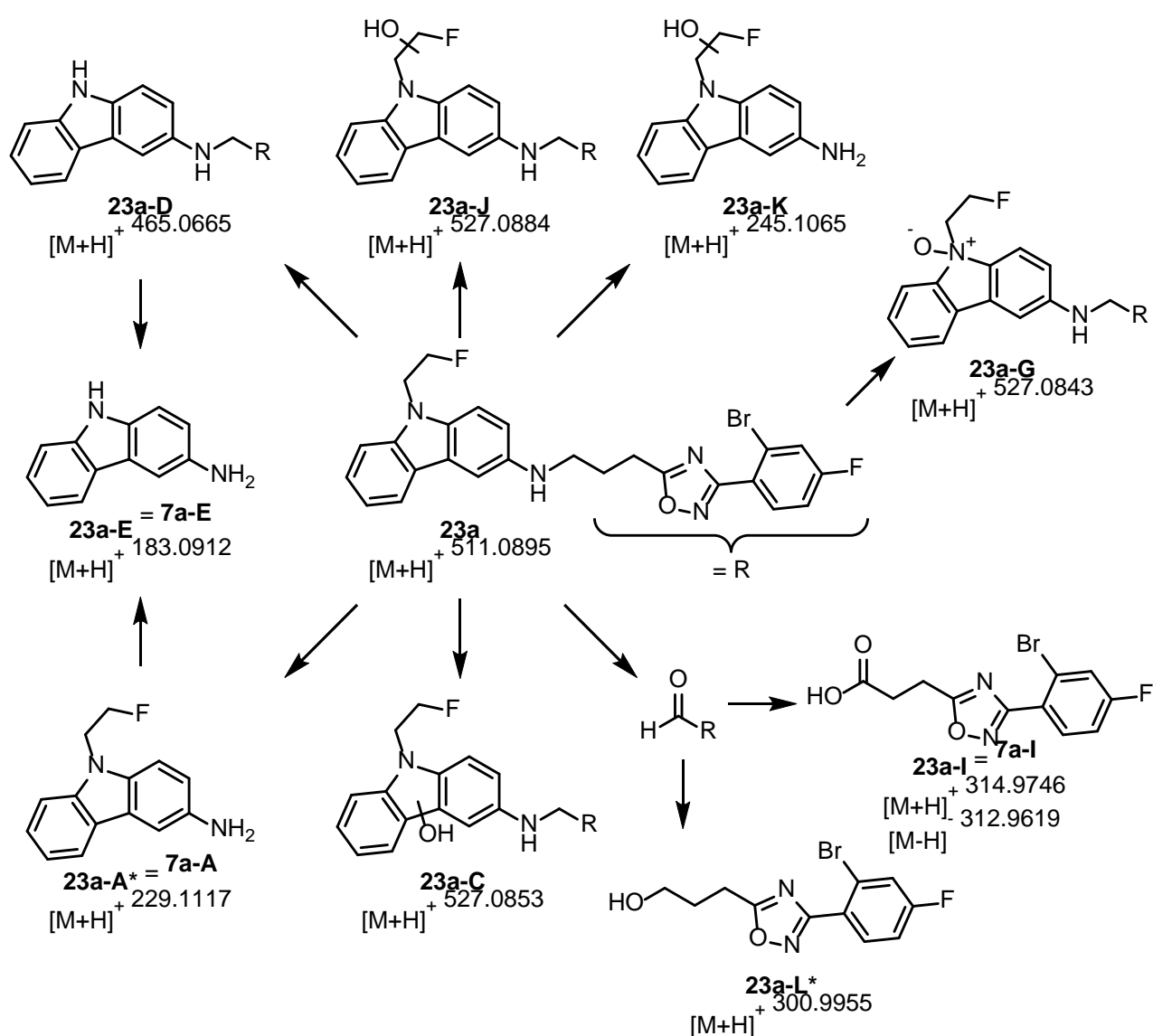


Figure 5. Proposed structures of metabolites identified 90 min after incubation of sec. amine **23a** with mouse liver microsomes and NADPH. * The marked metabolites were also formed without NADPH.

The pattern of metabolites formed upon incubation of secondary amine **23a** (Figure 5) is very similar to those formed from amide **7a**. The metabolites **23a-A** (**7a-A**), **23a-E** (**7a-E**) and **23a-I** (**7a-I**) formed upon oxidative *N*-dealkylation of **23a** are identical with the metabolites formed by amide hydrolysis of **7a**. Furthermore, the *N*-oxide **23a-G** was also formed and metabolites bearing an OH-moiety at the fluoroethyl side chain (**23a-J**) or in the carbazole system (**23a-C**) could be detected. The low stability of a possible hemiaminal led to the assumption, that the hydroxylation took place at the terminal carbon atom of the fluoroethyl residue (**23a-J**). Fragmentation of metabolite **23a-C** with an aromatic hydroxy moiety is given in Figure 6. Fragment m/z 257.1105 was obtained by β -cleavage at the secondary amine. Cleavage of the C-N bond led to fragment m/z 244.0994, which gave fragment m/z 198.0794 upon loss of the fluoroethyl side chain. All fragments contained an additional O-atom confirming the position of the additional OH-moiety at the carbazole system of metabolite **23a-C**.

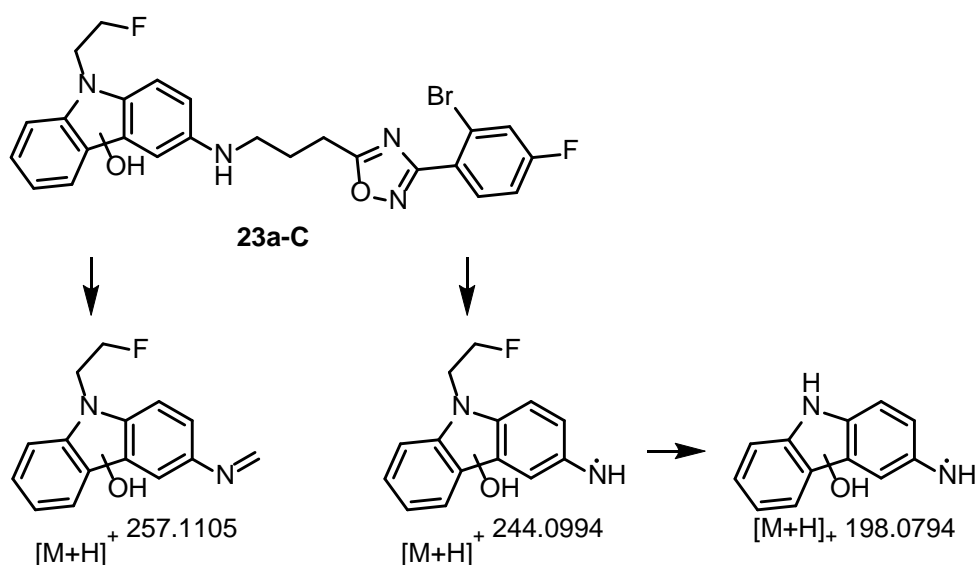


Figure 6. Fragmentation of metabolite **23a-C**.

The secondary amine **23a** was also cleaved in the presence and absence of NADPH, which resulted in the primary aromatic amine **23a-A**. It was assumed that the primary aliphatic alcohol **23a-L** was formed by reduction of the intermediate aldehyde, released upon oxidative *N*-dealkylation. Additionally, the aldehyde could also be oxidized to afford the carboxylic acid **23a-I**. However, the intermediate aldehyde could not be detected after incubation with and without NADPH. After incubation of **23a** with NADPH both metabolites, primary amine **23a-A** and alcohol **23a-L**, were formed in high amounts. Obviously, oxidative *N*-dealkylation plays an important role in the metabolism of secondary amine **23a**.

Serum stability was also determined for the secondary amine **23a** and the amide **7a**. With mouse serum, both CB₂ ligands were metabolized to the primary aromatic amine (**7a-A** = **23a-A**) (Figure 7). However, hydrolysis of amide **7a** gave larger amounts of primary amine **7a-A** than oxidative *N*-dealkylation of secondary amine **23a** after 90 min.

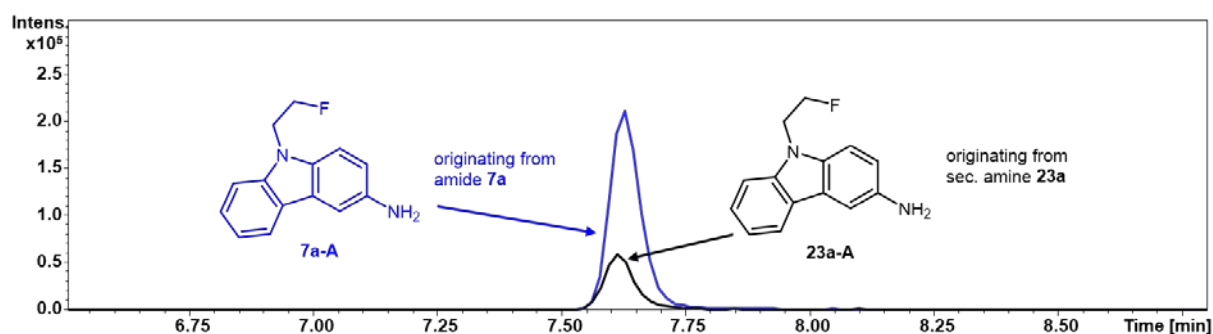


Figure 7. Incubation of amide **7a** and sec. amine **23a** with mouse serum. Comparison of the amount of formed primary amine **7a-A** = **23a-A** after 90 min.

After an incubation period of 90 min more than 98 % of parent ketone **26a** remained unchanged. Nevertheless, a few metabolites could be detected. Oxidative *N*-dealkylation (**26a-D**), hydroxylation of the fluoroethyl side chain (**26a-J**), as well as

hydroxylation of the carbazole moiety (**26a-C**) were observed. Moreover, the metabolite **26a-M** having an additional OH moiety in the butanone linker could be identified (Figure 8).

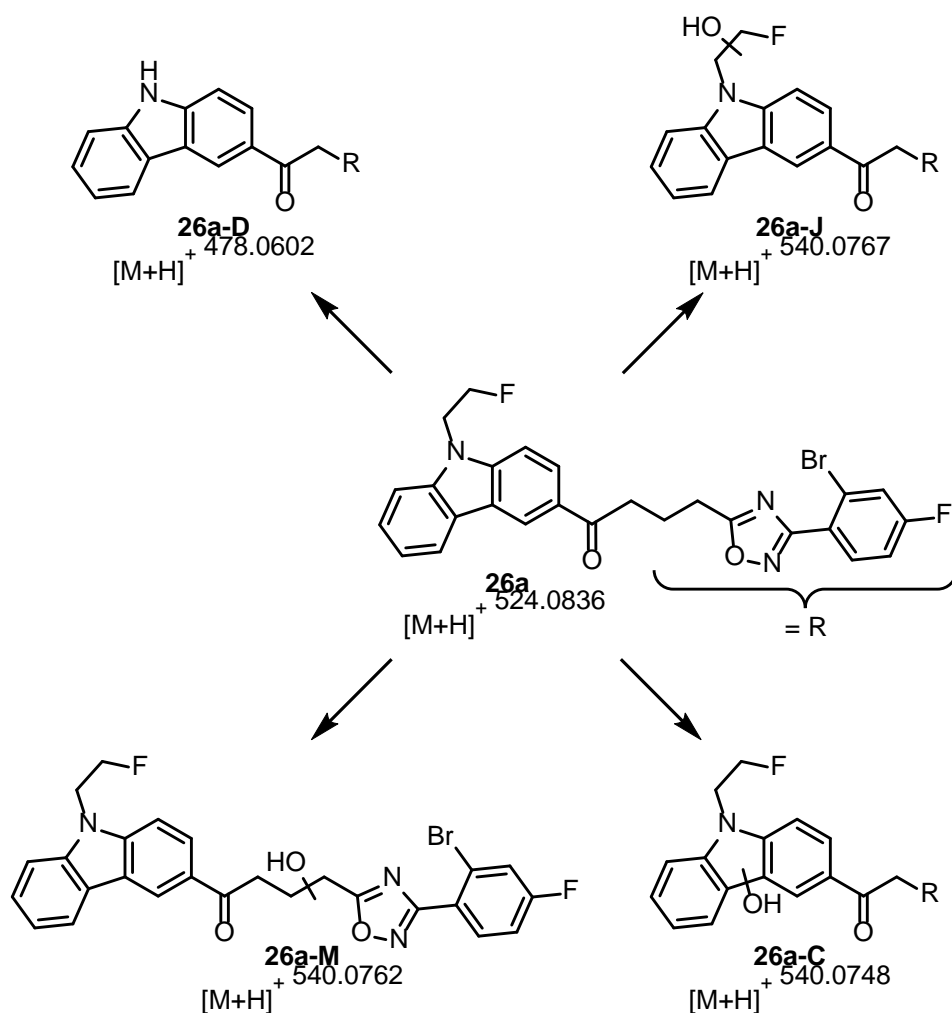


Figure 8. Proposed structures of metabolites identified 90 min after incubation of ketone **26a** with mouse liver microsomes and NADPH.

5. $\log D_{7.4}$ value determination of ketone **26a**

Another important parameter for the characterization of novel ligands is the lipophilicity. In this project, the $\log D_{7.4}$ value of the most promising compound **26a** was determined. For this purpose, the recently developed micro shake flask method in our lab was used and adapted to the high lipophilicity [36]. In this method an exact

amount of the respective compound was distributed between a defined volume of presaturated *n*-octanol and buffer (pH 7.4) layer. Afterwards, the concentration in the buffer layer was quantified by LC-quadrupole-MS with external calibration. Due to the high $\log D_{7.4}$ value of ketone **26a** and its poor ability to be ionized in ESI positive or negative mode, large amounts of the buffer phase had to be injected into the LC-MS. As a reversed phase column was used, ketone **26a** was trapped at the front of the column, which allowed multiple injections of the same sample prior to gradient elution. This procedure enabled detection of ketone **26a** in the subnanomolar range. The experimentally determined $\log D_{7.4}$ value of **26a** was 5.56 ± 0.08 . This value is higher than the reported $\log D$ value of **7a** ($\log D = 3.82 - 4.21$) [26], which was determined by a quite different method (correlation of HPLC retention times).

Calculation of $\log D_{7.4}$ values with ChemAxon[®], consensus mode, led to the following order of lipophilicity: ketone **26a** ($\text{clog} D_{7.4} = 6.76$) > secondary amine **23a** ($\text{clog} D_{7.4} = 6.62$) > amide **7a** ($\text{clog} D_{7.4} = 6.20$).

6. Conclusion

The aim of this study was the preparation of metabolically optimized CB₂ receptor ligands starting from the lead compound **7a**. In order to prevent the *in vivo* amide hydrolysis of **7a**, compounds with six alternative functional groups instead of the amide of **7a** were synthesized, which are non-hydrolysable or difficult to hydrolyze. The CB₂ and CB₁ receptor affinity of these compounds was determined by *in vitro* radioligand binding studies. Especially the alkanes **27a** ($K_i = 13$ nM) and **27b** ($K_i = 15$ nM), the secondary amines **23a** ($K_i = 7.9$ nM) and **23b** ($K_i = 7.1$ nM) as well as the ketones **26a** ($K_i = 8.6$ nM) and **26b** ($K_i = 11$ nM) show high CB₂ affinity. Furthermore, all tested compounds possess high CB₂:CB₁ selectivity. Since the

alkanes **27a** and **27b** were classified as too lipophilic, the secondary amine **23a** and ketone **26a** were examined in more detail concerning pharmacokinetic aspects. During *in vitro* incubations over 90 min with mouse liver microsomes, secondary amine **23a** was slightly and ketone **26a** was considerably more stable than amide **7a**. Further investigations of the formed metabolites demonstrated that the amide of the lead compound **7a** was hydrolyzed predominantly, whereas *N*-dealkylation of the secondary amine in the biotransformation of **23a** played a major role. Since more than 98 % of parent ketone **26a** remained unchanged after an incubation period of 90 min, the $\log D_{7.4}$ value was determined using the micro shake-flask method with LC-MS quantification. A $\log D_{7.4}$ value of 5.56 ± 0.08 was found for **26a**. The ketone **26a** is a promising starting point for the development of a promising PET tracer. As shown for the synthesis of [^{18}F]**7a** nucleophilic substitution of a tosylate precursor is envisaged to obtain [^{18}F]**26a**.

7. Experimental

7.1 Chemistry, General Methods

Oxygen and moisture sensitive reactions were carried out under nitrogen, dried with silica gel with moisture indicator (orange gel, Merck) and in dry glassware (Schlenk flask or Schlenk tube). Temperatures were controlled with dry ice/acetone (-78 °C), ice/water (0 °C), Cryostat (Julabo FT 901 or Huber TC100E-F), magnetic stirrer MR 3001 K (Heidolph) or RCT CL (IKA®), together with temperature controller EKT HeiCon (Heidolph) or VT-5 (VWR) and PEG or silicone bath. All solvents were of analytical grade quality. Demineralized water was used. THF was distilled from sodium/benzophenone. Methanol was distilled from magnesium methanolate. CH₃CN and ethanol abs. were dried with molecular sieves (3 Å); DMF, ethyl acetate and toluene were dried with molecular sieves (4 Å). Thin layer chromatography (tlc): tlc

silica gel 60 F₂₅₄ on aluminum sheets (Merck). Flash chromatography (fc): Silica gel 60, 40–63 μm (Merck); parentheses include: diameter of the column (\emptyset), length of the stationary phase (l), fraction size (v) and eluent. Melting point: Melting point system MP50 (Mettler Toledo), open capillary, uncorrected. MS: MicroTOFQII mass spectrometer (Bruker Daltonics); deviations of the found exact masses from the calculated exact masses were 5 ppm or less; the data were analyzed with DataAnalysis (Bruker). NMR: NMR spectra were recorded on Agilent DD2 400 MHz and 600 MHz spectrometers; chemical shifts (δ) are reported in parts per million (ppm) against the reference substance tetramethylsilane and calculated using the solvent residual peak of the undeuterated solvent. IR: FT/IR IRAffinity-1 IR spectrometer (Shimadzu) using ATR technique.

7.2 HPLC method for the determination of the purity

Equipment 1: Pump: L-7100, degasser: L-7614, autosampler: L-7200, UV detector: L-7400, interface: D-7000, data transfer: D-line, data acquisition: HSM-Software (all from LaChrom, Merck Hitachi); Equipment 2: Pump: LPG-3400SD, degasser: DG-1210, autosampler: ACC-3000T, UV-detector: VWD-3400RS, interface: DIONEX UltiMate 3000, data acquisition: Chromeleon 7 (Thermo Fisher Scientific); column: LiChropher[®] 60 RP-select B (5 μm), LiChroCART[®] 250-4 mm cartridge; flow rate: 1.0 mL/min; injection volume: 5.0 μL ; detection at $\lambda = 210 \text{ nm}$; solvents: A: demineralized water with 0.05 % (V/V) trifluoroacetic acid, B: acetonitrile with 0.05 % (V/V) trifluoroacetic acid; gradient elution (% A): 0 - 4 min: 90 %; 4 - 29 min: gradient from 90 % to 0 %; 29 - 31 min: 0 %; 31 - 31.5min: gradient from 0 % to 90 %; 31.5 - 40 min: 90 %. The purity of all compounds was determined by this method. With exception of compounds **23c**, **24c** and **28a**, the purity of all test compounds is higher

than 95 %.

7.3 Synthetic procedures

7.3.1 2-Bromo-4-fluorobenzamidoxime (**12**) [26]

Methanol (64 mL) was added to a stirred solution of $\text{NH}_2\text{OH}\cdot\text{HCl}$ (5.21 g, 75 mmol, 3 eq.) and Na_2CO_3 (3.98 g, 38 mmol, 1.5 eq.) in water (16 mL). After stirring for 20 min, 2-bromo-4-fluorobenzonitrile (**10**, 5.00 g, 25 mmol, 1 eq.) was added and the reaction mixture was heated at 86 °C for 20 h. The methanol was removed in vacuo and the aqueous suspension was diluted with ethyl acetate (100 mL). The organic layer was separated from the aqueous layer and washed with water (2 x 20 mL) and brine (20 mL). The combined aqueous layers were washed with ethyl acetate (2 x 50 mL). The combined ethyl acetate layers were dried (Na_2SO_4) and evaporated to dryness in vacuo. The residue was purified by fc ($\varnothing = 6.5$ cm, $l = 15$ cm, $v = 100$ mL, cyclohexane/ethyl acetate 60:40, $R_f = 0.34$ (cyclohexane/ethyl acetate 5:5)). Colorless solid, mp 120 - 121 °C, yield 3.43 g (59 %). Purity (HPLC): 96.4 % ($t_R = 3.7$ and 3.9 min). $\text{C}_7\text{H}_6\text{BrFN}_2\text{O}$ (233.0 g/mol). Exact mass (APCI): $m/z = 232.9722$ (calcd. 232.9720 for $\text{C}_7\text{H}_7^{79}\text{BrFN}_2\text{O}$ [$\text{M}+\text{H}^+$]). ^1H NMR (600 MHz, DMSO-D_6): δ (ppm) = 5.81 (s, 2H, NH_2), 7.28 (td, $J = 8.5/2.6$ Hz, 1H, 5-H), 7.42 (dd, $J = 8.5/6.2$ Hz, 1H, 6-H), 7.60 (dd, $J = 8.7/2.6$ Hz, 1H, 3-H), 9.45 (s, 1H, N-OH). ^{13}C NMR (101 MHz, DMSO-D_6): δ (ppm) = 114.5 (d, $J = 21.1$ Hz, 1C, C-5), 119.7 (d, $J = 24.7$ Hz, 1C, C-3), 122.6 (d, $J = 9.9$ Hz, 1C, C-2), 132.5 (d, $J = 3.5$ Hz, 1C, C-1), 132.7 (d, $J = 8.9$ Hz, 1C, C-6), 150.9 (1C, C=N), 161.7 (d, $J = 249.6$ Hz, 1C, C-4). FTIR (neat): $\tilde{\nu}$ (cm^{-1}) = 3483 (m, O-H), 3363 (m, N-H), 1664 (s, C=N), 1029 (m, C-Br, arom).

7.3.2 3-(2-Bromo-4-fluorophenyl)-5-(3-chloropropyl)-1,2,4-oxadiazole (**14**)

N-Ethyl-*N,N*-diisopropylamine (2.6 mL, 15 mmol, 2 eq.) and 4-chlorobutyryl chloride (0.85 mL, 7.6 mmol, 1 eq.) were added dropwise at 0 °C to a suspension of benzamidoxime **12** (1.78 g, 7.6 mmol, 1 eq.) in dry toluene (120 mL). The solution was stirred at room temperature for 6 h, followed by heating at reflux for 16 h. All volatiles were removed at reduced pressure and the residue was dissolved in ethyl acetate (350 mL). The solution was washed with water (2 x 80 mL) and brine (80 mL), dried (Na₂SO₄) and the organic layer was concentrated under reduced pressure. The residue was purified by fc (ϕ = 6 cm, *l* = 16 cm, *v* = 60 mL, cyclohexane/ethyl acetate 95:5, *R_f* = 0.71 (cyclohexane/ethyl acetate 3:7)). Colorless solid, mp 48 - 49 °C, yield 2.25 g (92 %). Purity (HPLC): 96.7 % (*t_R* = 22.7 min). C₁₁H₉BrClFN₂O (319.6 g/mol). Exact mass (APCI): *m/z* = 318.9659 (calcd. 318.9644 for C₁₁H₁₀⁷⁹Br³⁵ClFN₂O [M+H⁺]). ¹H NMR (400 MHz, DMSO-*D*₆): δ (ppm) = 2.26 (tt, *J* = 7.2/6.5 Hz, 2H, CH₂CH₂CH₂Cl), 3.17 (t, *J* = 7.4 Hz, 2H, CH₂CH₂CH₂Cl), 3.79 (t, *J* = 6.4 Hz, 2H, CH₂CH₂CH₂Cl), 7.47 (ddd, *J* = 8.7/8.2/2.6 Hz, 1H, 5-H), 7.84 (dd, *J* = 8.7/2.5 Hz, 1H, 3-H), 7.89 (dd, *J* = 8.7/6.1 Hz, 1H, 6-H). ¹³C NMR (151 MHz, DMSO-*D*₆): δ (ppm) = 23.2 (1C, CH₂CH₂CH₂Cl), 28.8 (1C, CH₂CH₂CH₂Cl), 44.0 (1C, CH₂CH₂CH₂Cl), 115.4 (d, *J* = 21.6 Hz, 1C, C-5), 121.3 (d, *J* = 25.0 Hz, 1C, C-3), 122.1 (d, *J* = 9.9 Hz, 1C, C-2), 124.4 (d, *J* = 3.6 Hz, 1C, C-1), 133.6 (d, *J* = 9.4 Hz, 1C, C-6), 162.8 (d, *J* = 253.3 Hz, 1C, C-4), 166.6 (1C, C-3_{oxadiazole}), 178.9 (1C, C-5_{oxadiazole}). FTIR (neat): $\tilde{\nu}$ (cm⁻¹) = 3078 (w, C-H, arom), 2958 (w, C-H, aliph), 1037 (m, C-Br, arom).

7.3.3 9-(2-Fluoroethyl)carbazole (**18**)

Under N₂ atmosphere, carbazole (**16**, 3.01 g, 18 mmol, 1 eq.) was dissolved in dry

DMF (80 mL) and cooled down to 0 °C. NaH (60 % dispersion in Paraffin Oil, 1.44 g, 36 mmol, 2 eq.) was added and the mixture was stirred for 30 min at 0 °C. After the dropwise addition of fluoroethyl tosylate (4.72 g, 22 mmol, 1.2 eq.), the mixture was stirred at room temperature for 19 h. Water (10 mL) and a saturated Na₂CO₃ solution (50 mL) were added and the mixture was extracted with CH₂Cl₂ (200 mL). The organic layer was washed with a saturated Na₂CO₃ solution (50 mL) and water (2 x 50 mL), dried (Na₂SO₄) and concentrated under reduced pressure. The residue was purified by fc ($\varnothing = 6.5$ cm, $l = 20$ cm, $v = 60$ mL, cyclohexane/ethyl acetate 99:1, $R_f = 0.51$ (cyclohexane/ethyl acetate 8:2)). Colorless solid, mp 85 °C, yield 2.83 g (74 %). Purity (HPLC): 97.1 % ($t_R = 22.7$ min). C₁₄H₁₂FN (213.3 g/mol). Exact mass (APCI): $m/z = 214.1036$ (calcd. 214.1027 for C₁₄H₁₃FN [M+H⁺]). ¹H NMR (400 MHz, CDCl₃): δ (ppm) = 4.58 (dt, $J = 23.9/5.2$ Hz, 2H, CH₂CH₂F), 4.79 (dt, $J = 46.8/5.3$ Hz, 2H, CH₂F), 7.23 - 7.29 (m, 2H, 3-H, 6-H), 7.41 (d, $J = 7.9$ Hz, 2H, 1-H, 8-H), 7.47 (ddd, $J = 8.2/7.0/1.2$ Hz, 2H, 2-H, 7-H), 8.11 (dt, $J = 7.8/0.8$ Hz, 2H, 4-H, 5-H). ¹³C NMR (101 MHz, CDCl₃): δ (ppm) = 43.5 (d, $J = 22.9$ Hz, 1C, CH₂CH₂F), 82.0 (d, $J = 172.8$ Hz, 1C, CH₂F), 108.7 (d, $J = 1.2$ Hz, 2C, C-1, C-8), 119.5 (2C, C-3, C-6), 120.5 (2C, C-4, C-5), 123.2 (2C, C-4a, C-4b), 126.0 (2C, C-2, C-7), 140.6 (2C, C-8a, C-9a). FTIR (neat): $\tilde{\nu}$ (cm⁻¹) = 3047 (w, C-H, arom), 2947 (w, C-H, aliph), 1593 (m, C-C, arom).

7.3.4 9-(2-Fluoroethyl)-3-nitrocarbazole (**20**)

Fluoroethylcarbazole **18** (2.57 g, 12 mmol, 1 eq.) was dissolved in CH₂Cl₂ (62 mL) and cooled down to 0 °C. HNO₃ 65 % (1.2 mL, 18 mmol, 1.5 eq.) was added dropwise over 30 min and the solution was stirred at 0 °C for another 3 h. Afterwards, the reaction mixture was diluted with water (15 mL), neutralized with a saturated

NaHCO₃ solution and the aqueous layer was diluted with water to 80 mL. After evaporation of CH₂Cl₂ in vacuo, the aqueous layer was extracted with ethyl acetate (4 x 200 mL). The combined organic layers were dried (Na₂SO₄) and concentrated in vacuo. The residue was purified by fc with a gradient (ϕ = 5 cm, l = 15 cm, v = 60 mL, cyclohexane/ethyl acetate 70:30, 50:50, 0:100, R_f = 0.64 (cyclohexane/ethyl acetate 5:5)). Yellow solid, mp 191 - 192 °C, yield 2.50 g (80 %). Purity (HPLC): 98.7 % (t_R = 22.7 min). C₁₄H₁₁FN₂O₂ (258.3 g/mol). Exact mass (APCI): m/z = 259.0885 (calcd. 259.0877 for C₁₄H₁₂FN₂O₂ [M+H⁺]). ¹H NMR (400 MHz, CDCl₃): δ (ppm) = 4.66 (dt, *J* = 25.3/4.9 Hz, 2H, CH₂CH₂F), 4.85 (dt, *J* = 46.7/5.0 Hz, 2H, CH₂F), 7.34 - 7.43 (m, 1H, 6-H), 7.42 - 7.51 (m, 2H, 1-H, 8-H), 7.58 (ddd, *J* = 8.3/7.1/1.1 Hz, 1H, 7-H), 8.17 (dd, *J* = 7.8/1.0 Hz, 1H, 5-H), 8.39 (dd, *J* = 9.1/2.2 Hz, 1H, 2-H), 9.01 (d, *J* = 2.2 Hz, 1H, 4-H). ¹³C NMR (151 MHz, CDCl₃): δ (ppm) = 44.1 (d, *J* = 22.1 Hz, 1C, CH₂CH₂F), 81.8 (d, *J* = 173.4 Hz, 1C, CH₂F), 108.6 (d, *J* = 2.1 Hz, 1C, C-1), 109.6 (d, *J* = 1.0 Hz, 1C, C-8), 117.4 (1C, C-4), 121.2 (1C, C-5), 121.4 (1C, C-6), 121.9 (1C, C-2), 123.0 (1C, C-4a), 123.2 (1C, C-4b), 127.8 (1C, C-7), 141.2 (1C, C-3), 141.7 (1C, C-8a), 143.9 (1C, C-9a). FTIR (neat): $\tilde{\nu}$ (cm⁻¹) = 3055 (w, C-H, arom), 2920, 2850 (w, C-H, aliph), 1307 (s, NO₂).

7.3.5 9-(2-Fluoroethyl)carbazol-3-ammonium chloride (**22**·HCl)

Under N₂ atmosphere, nitrocarbazole **20** (2.50 g, 9.7 mmol, 1 eq.) was dissolved in dry THF (260 mL). Pd/C 10 % (0.375 g) was added and the mixture was stirred for 23 h under H₂ atmosphere (balloon). After filtration through Celite[®], the solvent was removed under reduced pressure and the residue was dissolved in Et₂O (300 mL). A solution of HCl in Et₂O (2 M, 5.0 mL, 10 mmol, 1.03 eq.) was added dropwise until the salt **22**·HCl precipitated completely. The precipitate was filtered off, washed with

cold Et₂O and dried under reduced pressure. R_f = 0.61 (cyclohexane/ethyl acetate 3:7). Grey solid, mp 230 - 253 °C (decomposition), yield 2.41 g (94 %). Purity (HPLC): 95.9 % (t_R = 15.2 min). C₁₄H₁₄ClFN₂ (264.7 g/mol). Exact mass (APCI): m/z = 229.1135 (calcd. 229.1136 for C₁₄H₁₄ClFN₂ [M+H⁺]). ¹H NMR (400 MHz, DMSO-D₆): δ (ppm) = 4.72 - 4.87 (m, 4H, CH₂CH₂F), 7.23 - 7.28 (m, 1H, 6-H), 7.48 - 7.54 (m, 2H, 2-H, 7-H), 7.68 (d, J = 8.3 Hz, 1H, 8-H), 7.75 (d, J = 8.7 Hz, 1H, 1-H), 8.16 (d, J = 2.1 Hz, 1H, 4-H), 8.19 (d, J = 7.8 Hz, 1H, 5-H), 10.52 (s, 3H, -NH₃⁺). ¹³C NMR (101 MHz, DMSO-D₆): δ (ppm) = 43.5 (d, J = 20.0 Hz, 1C, CH₂CH₂F), 83.0 (d, J = 167.7 Hz, 1C, CH₂F), 110.4 (1C, C-8), 110.9 (1C, C-1), 115.2 (1C, C-4), 120.0 (1C, C-6), 121.0 (1C, C-5), 121.2 (1C, C-2), 121.9 (1C, C-4b), 122.8 (1C, C-4a), 123.6 (1C, C-3), 127.07 (1C, C-7), 139.8 (1C, C-9a), 141.3 (1C, C-8a). FTIR (neat): $\tilde{\nu}$ (cm⁻¹) = 3051 (w, C-H, arom), 2843 (m, C-H, aliph).

7.3.6 *N*-{3-[3-(2-Bromo-4-fluorophenyl)-1,2,4-oxadiazol-5-yl]propyl}-9-(2-fluoroethyl)carbazol-3-amine (**23a**)

Under N₂ atmosphere, triethylamine (0.20 mL, 1.5 mmol, 3 eq.), chloroalkane **14** (156 mg, 0.49 mmol, 1 eq.) and tetrabutylammonium iodide (181 mg, 0.49 mmol, 1 eq.) were sequentially added to a suspension of carbazolumine hydrochloride **22**·HCl (144 mg, 0.54 mmol, 1.1 eq.) in dry toluene (20 mL). After the reaction mixture was heated at reflux for 68 h, the cold mixture was filtered and all volatiles were removed under reduced pressure. The residue was dissolved in ethyl acetate (40 mL). Afterwards, the organic layer was washed with HCl solution (1 M, 15 mL) and water (2 x 15 mL), dried (Na₂SO₄) and concentrated in vacuo. The residue was purified by fc (∅ = 2 cm, l = 17 cm, v = 10 mL, cyclohexane/ethyl acetate/dimethylethylamine 85:15:3, R_f = 0.64 (cyclohexane/ethyl acetate 6:4)).

Brown solid, mp 103 °C, yield 137 mg (55 %). Purity (HPLC): 96.2 % (t_R = 20.9 min). $C_{25}H_{21}BrF_2N_4O$ (511.4 g/mol). Exact mass (APCI): m/z = 511.0915 (calcd. 511.0940 for $C_{25}H_{22}^{79}BrF_2N_4O$ [$M+H^+$]). 1H NMR (400 MHz, DMSO- D_6): δ (ppm) = 2.15 (quint, J = 7.1 Hz, 2H, $NCH_2CH_2CH_2$), 3.19 (t, J = 7.4 Hz, 2H, $NCH_2CH_2CH_2$), 3.27 (t, J = 6.8 Hz, 2H, $NCH_2CH_2CH_2$), 4.61 (dt, J = 27.3/4.6 Hz, 2H, CH_2CH_2F), 4.74 (dt, J = 47.4/4.6 Hz, 2H, CH_2F), 5.45 (s, 1H, NH), 6.86 (dd, J = 8.7/2.2 Hz, 1H, 8- H_{carb}), 7.06 (t, J = 7.4 Hz, 1H, 6- H_{carb}), 7.28 (d, J = 2.1 Hz, 1H, 4- H_{carb}), 7.32 - 7.38 (m, 2H, 2- H_{carb} , 7- H_{carb}), 7.43 (td, J = 8.4/2.6 Hz, 1H, 5- H_{phenyl}), 7.49 (d, J = 8.2 Hz, 1H, 1- H_{carb}), 7.82 - 7.89 (m, 2H, 3- H_{phenyl} , 6- H_{phenyl}), 7.96 (d, J = 7.7 Hz, 1H, 5- H_{carb}). ^{13}C NMR (101 MHz, DMSO- D_6): δ (ppm) = 23.6 (1C, $NCH_2CH_2CH_2$), 25.5 (1C, $NCH_2CH_2CH_2$), 42.9 (d, J = 20.4 Hz, 1C, CH_2CH_2F), 43.1 (1C, $NCH_2CH_2CH_2$), 82.6 (d, J = 167.9 Hz, 1C, CH_2F), 101.5 (1C, C-4 $_{carb}$), 109.2 (1C, C-1 $_{carb}$), 110.0 (1C, C-2 $_{carb}$), 114.6 (1C, C-8 $_{carb}$), 115.4 (d, J = 21.6 Hz, 1C, C-5 $_{phenyl}$), 117.9 (1C, C-6 $_{carb}$), 120.0 (1C, C-5 $_{carb}$), 121.3 (d, J = 25.1 Hz, 1C, C-3 $_{phenyl}$), 122.1 (1C, C-4 $_{bcarb}$), 122.2 (d, J = 10.2 Hz, 1C, C-2 $_{phenyl}$), 122.9 (1C, C-4 $_{a_{carb}}$), 124.6 (d, J = 3.5 Hz, 1C, C-1 $_{phenyl}$), 125.1 (1C, C-7 $_{carb}$), 133.4 (1C, C-9 $_{a_{carb}}$), 133.6 (d, J = 9.4 Hz, 1C, C-6 $_{phenyl}$), 140.4 (1C, C-8 $_{a_{carb}}$), 142.3 (1C, C-3 $_{carb}$), 162.9 (d, J = 253.3 Hz, 1C, C-4 $_{phenyl}$), 166.7 (1C, C-3 $_{oxadiazole}$), 180.0 (1C, C-5 $_{oxadiazole}$). FTIR (neat): $\tilde{\nu}$ (cm^{-1}) = 3379 (w, N-H), 3055 (w, C-H, arom), 2935 (w, C-H, aliph), 1593 (m, C-C, arom), 1573 (m, C-C, arom).

7.3.7 *N*-{3-[3-(2-Bromo-4-fluorophenyl)-1,2,4-oxadiazol-5-yl]propyl}-9-(2-fluoroethyl)-*N*-methylcarbazol-3-amine (**24a**)

Under N_2 atmosphere, triethylamine (0.16 mL, 1.1 mmol, 3 eq.) and iodomethane (0.24 mL, 3.8 mmol, 10 eq.) were added to a solution of secondary amine **23a** (195 mg, 0.38 mmol, 1 eq.) in dry CH_3CN (20 mL). After the reaction mixture was heated at reflux for 2.75 h, the cold mixture was filtered and all volatiles were

removed in vacuo. The residue was dissolved in ethyl acetate (20 mL) and the mixture was washed with HCl solution (1 M, 10 mL) and water (3 x 10 mL). Afterwards, the organic layer was dried (Na_2SO_4) and concentrated in vacuo. The residue was purified by fc ($\phi = 2$ cm, $l = 20$ cm, $v = 10$ mL, cyclohexane/ethyl acetate/dimethylethylamine 92:8:3, $R_f = 0.73$ (cyclohexane/ethyl acetate 6:4)). Brown resin, yield 73 mg (37 %). Purity (HPLC): 95.8 % ($t_R = 21.2$ min). $\text{C}_{26}\text{H}_{23}\text{BrF}_2\text{N}_4\text{O}$ (525.4 g/mol). Exact mass (APCI): $m/z = 525.1082$ (calcd. 525.1096 for $\text{C}_{26}\text{H}_{24}^{79}\text{BrF}_2\text{N}_4\text{O} [\text{M}+\text{H}^+]$). ^1H NMR (400 MHz, CDCl_3): δ (ppm) = 2.23 (quint, $J = 7.2$ Hz, 2H, $\text{NCH}_2\text{CH}_2\text{CH}_2$), 3.01 (s, 3H, NCH_3), 3.08 (t, $J = 7.3$ Hz, 2H, $\text{NCH}_2\text{CH}_2\text{CH}_2$), 3.51 (t, $J = 6.3$ Hz, 2H, $\text{NCH}_2\text{CH}_2\text{CH}_2$), 4.55 (dt, $J = 23.7/4.7$ Hz, 2H, $\text{CH}_2\text{CH}_2\text{F}$), 4.77 (dt, $J = 46.8/5.2$ Hz, 2H, CH_2F), 7.05 - 7.13 (m, 2H, 5- H_{phenyl} , 2- H_{carb}), 7.17 (t, $J = 7.4$ Hz, 1H, 6- H_{carb}), 7.30 (d, $J = 8.8$ Hz, 1H, 1- H_{carb}), 7.35 (d, $J = 8.1$ Hz, 1H, 8- H_{carb}), 7.40 - 7.45 (m, 1H, 7- H_{carb}), 7.47 (dd, $J = 8.2/2.6$ Hz, 1H, 3- H_{phenyl}), 7.50 - 7.56 (m, 1H, 4- H_{carb}), 7.80 (dd, $J = 8.7/6.0$ Hz, 1H, 6- H_{phenyl}), 8.01 (d, $J = 7.8$ Hz, 1H, 5- H_{carb}). ^{13}C NMR (101 MHz, CDCl_3): δ (ppm) = 24.0 (1C, $\text{NCH}_2\text{CH}_2\text{CH}_2$), 24.3 (1C, $\text{NCH}_2\text{CH}_2\text{CH}_2$), 40.6 (1C, NCH_3), 43.6 (d, $J = 22.8$ Hz, 1C, $\text{CH}_2\text{CH}_2\text{F}$), 54.2 (1C, $\text{NCH}_2\text{CH}_2\text{CH}_2$), 82.1 (d, $J = 172.6$ Hz, 1C, CH_2F), 106.3 (1C, C-4 $_{\text{carb}}$), 108.6 (1C, C-8 $_{\text{carb}}$), 109.3 (1C, C-1 $_{\text{carb}}$), 115.0 (d, $J = 21.4$ Hz, 1C, C-5 $_{\text{phenyl}}$), 115.9 (1C, C-2 $_{\text{carb}}$), 118.9 (1C, C-6 $_{\text{carb}}$), 120.5 (1C, C-5 $_{\text{carb}}$), 121.7 (d, $J = 24.7$ Hz, 1C, C-3 $_{\text{phenyl}}$), 122.9 (d, $J = 9.7$ Hz, 1C, C-2 $_{\text{phenyl}}$), 123.0 (1C, C-4b $_{\text{carb}}$), 123.9 (1C, C-4a $_{\text{carb}}$), 124.8 (d, $J = 3.6$ Hz, 1C, C-1 $_{\text{phenyl}}$), 125.9 (1C, C-7 $_{\text{carb}}$), 133.4 (d, $J = 9.1$ Hz, 1C, C-6 $_{\text{phenyl}}$), 134.9 (1C, C-9a $_{\text{carb}}$), 141.1 (1C, C-8a $_{\text{carb}}$), 144.1 (1C, C-3 $_{\text{carb}}$), 163.4 (d, $J = 255.5$ Hz, 1C, C-4 $_{\text{phenyl}}$), 167.3 (1C, C-3 $_{\text{oxadiazole}}$), 179.4 (1C, C-5 $_{\text{oxadiazole}}$). FTIR (neat): $\tilde{\nu}$ (cm^{-1}) = 3051 (w, C-H, arom), 2947 (w, C-H, aliph), 1600 (m, C-C, arom), 1573 (m, C-C, arom).

7.3.8 5-[9-(2-Fluoroethyl)carbazol-3-yl]-5-oxopentanoic acid (**25**)

Under N₂ atmosphere, BF₃·Et₂O (78.5 mL, 620 mmol, 33 eq.) was added to a mixture of 4-(methoxycarbonyl)butanoyl chloride (3.9 mL, 28 mmol, 1.5 eq.) and fluoroethylcarbazole **18** (4.00 g, 19 mmol, 1 eq.). The mixture was heated at 50 °C. After 2 h, additional acid chloride (1.3 mL, 9.4 mmol, 0.5 eq.) was added at room temperature and the reaction mixture was heated at 50 °C for another 19 h. At 0 °C NaOH solution (20 %, 320 mL) was slowly added to the reaction mixture (violent reaction). The organic solvent was evaporated in vacuo and methanol (250 mL) was added dropwise at 0 °C. Stirring was continued at room temperature for 74 h. Afterwards, methanol was removed in vacuo and the pH value was adjusted to 1 with HCl 37 %. The resulting suspension was filtered and washed with 50 °C warm ethyl acetate (200 mL). The aqueous layer was extracted with ethyl acetate (2 x 200 mL). The combined organic layers were washed with brine (100 mL), dried (Na₂SO₄) and the solvent was evaporated in vacuo. The residue was purified by fc with a gradient ($\emptyset = 6$ cm, $l = 18$ cm, $v = 60$ mL, cyclohexane/ethyl acetate/formic acid 80:20:0.5, 65:35:0.5, 50:50:0.5, $R_f = 0.50$ (cyclohexane/ethyl acetate/formic acid 5:5:0.2)). The product was purified by recrystallization (ethyl acetate). Beige solid, mp 152 °C, yield 1.92 g (31 %). Purity (HPLC): 96.1 % ($t_R = 19.6$ min). C₁₉H₁₈FNO₃ (327.4 g/mol). Exact mass (APCI): $m/z = 328.1347$ (calcd. 328.1343 for C₁₉H₁₉FNO₃ [M+H⁺]). ¹H NMR (400 MHz, DMSO-D₆): δ (ppm) = 1.92 (quint, $J = 7.3$ Hz, 2H, CH₂CH₂CH₂CO₂H), 2.37 (t, $J = 7.4$ Hz, 2H, CH₂CH₂CH₂CO₂H), 3.18 (t, $J = 7.3$ Hz, 2H, CH₂CH₂CH₂CO₂H), 4.73 - 4.90 (m, 4H, CH₂CH₂F), 7.30 (t, $J = 7.4$ Hz, 1H, 6-H), 7.51 (ddd, $J = 8.3/7.1/1.2$ Hz, 1H, 7-H), 7.65 - 7.74 (m, 2H, 1-H, 8-H), 8.08 (dd, $J = 8.7/1.6$ Hz, 1H, 2-H), 8.31 (d, $J = 7.7$ Hz, 1H, 5-H), 8.88 (d, $J = 1.3$ Hz, 1H, 4-H). ¹³C NMR (101 MHz, DMSO-D₆): δ (ppm) = 19.8 (1C, CH₂CH₂CO₂H), 33.0 (1C,

CH₂CO₂H), 37.1 (1C, CH₂CH₂CH₂CO₂H), 43.1 (d, *J* = 20.1 Hz, 1C, CH₂CH₂F), 82.5 (d, *J* = 167.9 Hz, 1C, CH₂F), 109.4 (1C, C-1), 110.1 (1C, C-8), 120.0 (1C, C-6), 120.7 (1C, C-5), 121.4 (1C, C-4), 122.0 (1C, C-4a), 122.6 (1C, C-4b), 125.8 (1C, C-2), 126.5 (1C, C-7), 128.4 (1C, C-3), 140.9 (1C, C-8a), 142.9 (1C, C-9a), 174.4 (1C, CO₂H), 198.7 (1C, C=O). FTIR (neat): $\tilde{\nu}$ (cm⁻¹) = 3250 - 2300 (b, O-H), 1712 (s, C=O), 1670 (m, C=O).

7.3.9 4-[3-(2-Bromo-4-fluorophenyl)-1,2,4-oxadiazol-5-yl]-1-[9-(2-fluoroethyl)carbazol-3-yl]butan-1-one (**26a**)

Under N₂ atmosphere, *N*-ethyl-*N,N*-diisopropylamine (66 μ L, 0.38 mmol, 2 eq.) and COMU[®] (106 mg, 0.25 mmol, 1.3 eq.) were added to a solution of carboxylic acid **25** (71 mg, 0.21 mmol, 1.1 eq.) in dry THF (2.5 mL). After the reaction mixture was stirred at room temperature for 30 min, it was cooled down to 0 °C and benzamidoxime **12** (45 mg, 0.19 mmol, 1 eq.) was added. Stirring was continued at room temperature for 24 h. Afterwards, THF was removed in vacuo, dry toluene (2 mL) was added and the mixture was heated at reflux for 24 h. All volatiles were removed under reduced pressure and the residue was dissolved in ethyl acetate (30 mL). The organic layer was washed with water (2 x 10 mL) and brine (10 mL), dried (Na₂SO₄) and concentrated in vacuo. The residue was purified by fc with a gradient (\emptyset = 2 cm, *l* = 15 cm, *v* = 10 mL, cyclohexane/ethyl acetate 85:15, 75:25, *R_f* = 0.50 (cyclohexane/ethyl acetate 6:4)). Beige solid, mp 150 °C, yield 61 mg (61 %). Purity (HPLC): 96.0 % (*t_R* = 25.2 min). C₂₆H₂₀BrF₂N₃O₂ (524.3 g/mol). Exact mass (APCI): *m/z* = 524.0755 (calcd. 524.0780 for C₂₆H₂₁⁷⁹BrF₂N₃O₂ [M+H⁺]). ¹H NMR (400 MHz, DMSO-*D*₆): δ (ppm) = 2.22 (quint, *J* = 7.2 Hz, 2H, COCH₂CH₂CH₂), 3.17 (t, *J* = 7.4 Hz, 2H, COCH₂CH₂CH₂), 3.36 (t, *J* = 7.1 Hz, 2H, COCH₂CH₂CH₂),

4.72 - 4.91 (m, 4H, CH₂CH₂F), 7.29 (t, *J* = 7.5 Hz, 1H, 6-H_{carb}), 7.43 (td, *J* = 8.4/2.5 Hz, 1H, 5-H_{phenyl}), 7.52 (t, *J* = 7.6 Hz, 1H, 7-H_{carb}), 7.68 - 7.74 (m, 2H, 1-H_{carb}, 8-H_{carb}), 7.82 (dd, *J* = 8.6/2.5 Hz, 1H, 3-H_{phenyl}), 7.88 (dd, *J* = 8.7/6.1 Hz, 1H, 6-H_{phenyl}), 8.10 (dd, *J* = 8.8/1.4 Hz, 1H, 2-H_{carb}), 8.27 (d, *J* = 7.7 Hz, 1H, 5-H_{carb}), 8.89 (d, *J* = 1.4 Hz, 1H, 4-H_{carb}). ¹³C NMR (101 MHz, DMSO-D₆): δ (ppm) = 21.0 (1C, COCH₂CH₂CH₂), 25.2 (1C, COCH₂CH₂CH₂), 36.6 (1C, COCH₂CH₂CH₂), 43.1 (d, *J* = 19.9 Hz, 1C, CH₂CH₂F), 82.5 (d, *J* = 167.8 Hz, 1C, CH₂F), 109.4 (1C, C-1_{carb}), 110.1 (1C, C-8_{carb}), 115.4 (d, *J* = 21.6 Hz, 1C, C-5_{phenyl}), 120.0 (1C, C-6_{carb}), 120.6 (1C, C-5_{carb}), 121.3 (d, *J* = 25.1 Hz, 1C, C-3_{phenyl}), 121.5 (1C, C-4_{carb}), 122.0 (1C, C-4_acarb), 122.2 (d, *J* = 10.1 Hz, 1C, C-2_{phenyl}), 122.5 (1C, C-4_bcarb), 124.5 (d, *J* = 3.5 Hz, 1C, C-1_{phenyl}), 125.8 (1C, C-2_{carb}), 126.5 (1C, C-7_{carb}), 128.3 (1C, C-3_{carb}), 133.6 (d, *J* = 9.4 Hz, 1C, C-6_{phenyl}), 140.9 (1C, C-8_acarb), 143.0 (1C, C-9_acarb), 162.8 (d, *J* = 253.3 Hz, 1C, C-4_{phenyl}), 166.6 (1C, C-3_{oxadiazole}), 179.7 (1C, C-5_{oxadiazole}), 198.3 (1C, C=O). FTIR (neat): $\tilde{\nu}$ (cm⁻¹) = 2935 (w, C-H, aliph), 1666 (m, C=O), 1593 (m, C-C, arom), 1573 (m, C-C, arom).

7.3.10 3-{4-[3-(2-Bromo-4-fluorophenyl)-1,2,4-oxadiazol-5-yl]butyl}-9-(2-fluoroethyl)carbazole (27a)

Et₃SiH (78 μL, 0.49 mmol, 2.5 eq.) was added dropwise to a solution of ketone **26a** (103 mg, 0.20 mmol, 1 eq.) in trifluoroacetic acid (0.80 mL). After the reaction mixture was heated at 55 °C for 3 h, the mixture was carefully dropped into water (10 mL) at 0 °C and the mixture was neutralized with NaOH. The aqueous suspension was extracted with ethyl acetate (3 x 10 mL). Afterwards, the organic layer was washed with water (10 mL) and brine (10 mL), dried (Na₂SO₄) and concentrated in vacuo. The residue was purified by fc (∅ = 2 cm, l = 15 cm, v = 10 mL, cyclohexane/ethyl acetate 90:10, R_f = 0.73 (cyclohexane/ethyl acetate 6:4)). Brownish resin, yield

77 mg (77 %). Purity (HPLC): 97.4 % ($t_R = 27.9$ min). $C_{26}H_{22}BrF_2N_3O$ (510.4 g/mol). Exact mass (APCI): $m/z = 510.0988$ (calcd. 510.0987 for $C_{26}H_{23}^{79}BrF_2N_3O$ [$M+H^+$]). 1H NMR (400 MHz, $CDCl_3$): δ (ppm) = 1.83 - 1.93 (m, 2H, C-3_{carb}- $CH_2CH_2CH_2CH_2$), 1.93 - 2.02 (m, 2H, C-3_{carb}- $CH_2CH_2CH_2CH_2$), 2.88 (t, $J = 7.4$ Hz, 2H, C-3_{carb}- $CH_2CH_2CH_2CH_2$), 3.02 (t, $J = 7.4$ Hz, 2H, C-3_{carb}- $CH_2CH_2CH_2CH_2$), 4.59 (dt, $J = 23.8/5.2$ Hz, 2H, CH_2CH_2F), 4.79 (dt, $J = 46.8/5.2$ Hz, 2H, CH_2F), 7.10 - 7.15 (m, 1H, 5- H_{phenyl}), 7.21 - 7.26 (m, 1H, 6- H_{carb}), 7.30 (dd, $J = 8.4/1.6$ Hz, 1H, 2- H_{carb}), 7.34 (d, $J = 8.3$ Hz, 1H, 1- H_{carb}), 7.39 (d, $J = 8.1$ Hz, 1H, 8- H_{carb}), 7.43 - 7.49 (m, 2H, 3- H_{phenyl} , 7- H_{carb}), 7.83 (dd, $J = 8.7/6.0$ Hz, 1H, 6- H_{phenyl}), 7.90 (d, $J = 0.6$ Hz, 1H, 4- H_{carb}), 8.07 (d, $J = 7.8$ Hz, 1H, 5- H_{carb}). ^{13}C NMR (101 MHz, $CDCl_3$): δ (ppm) = 26.3 (1C, C-3_{carb}- $CH_2CH_2CH_2CH_2$), 26.6 (1C, C-3_{carb}- $CH_2CH_2CH_2CH_2$), 31.6 (1C, C-3_{carb}- $CH_2CH_2CH_2CH_2$), 35.5 (1C, C-3_{carb}- $CH_2CH_2CH_2CH_2$), 43.5 (d, $J = 22.8$ Hz, 1C, CH_2CH_2F), 82.0 (d, $J = 172.7$ Hz, 1C, CH_2F), 108.5 (d, $J = 1.1$ Hz, 1C, C-1_{carb}), 108.6 (d, $J = 1.0$ Hz, 1C, C-8_{carb}), 115.0 (d, $J = 21.4$ Hz, 1C, C-5_{phenyl}), 119.4 (1C, C-6_{carb}), 120.0 (1C, C-4_{carb}), 120.5 (1C, C-5_{carb}), 121.7 (d, $J = 24.7$ Hz, 1C, C-3_{phenyl}), 122.9 (d, $J = 9.8$ Hz, 1C, C-2_{phenyl}), 123.1 (1C, C-4_{bcarb}), 123.4 (1C, C-4_{acarb}), 124.8 (d, $J = 3.5$ Hz, 1C, C-1_{phenyl}), 125.9 (1C, C-7_{carb}), 126.7 (1C, C-2_{carb}), 132.9 (1C, C-3_{carb}), 133.4 (d, $J = 9.1$ Hz, 1C, C-6_{phenyl}), 139.2 (1C, C-9_{acarb}), 140.9 (1C, C-8_{acarb}), 163.4 (d, $J = 255.6$ Hz, 1C, C-4_{phenyl}), 167.3 (1C, C-3_{oxadiazole}), 179.7 (1C, C-5_{oxadiazole}). FTIR (neat): $\tilde{\nu}$ (cm^{-1}) = 2924 (w, C-H, aliph), 1600 (m, C-C, arom), 1570 (m, C-C, arom).

7.4 Receptor binding studies to determine CB_1 and CB_2 receptor affinity

$[^3H]$ CP55940 displacement assays were used for the determination of affinity (K_i) values of ligands for the cannabinoid CB_1 and CB_2 receptors. Membrane aliquots containing 5 μg (CHOK1h CB_1 _bgal) or 1 μg (CHOK1h CB_2 _bgal) of membrane protein in 100 μL assay buffer (50 mM Tris-HCl, 5 mM $MgCl_2$, 0.1 % BSA, pH 7.4)

were incubated at 30 °C for 1 h, in presence of 3.5 nM [³H]CP55940 (CHOK1hCB₁_bgal) or 1.5 nM [³H]CP55940 (CHOK1hCB₂_bgal). Initially, 1 μM of competing ligand was used, followed by six concentrations of competing ligand (between 10^{-5.5} M and 10^{-10.5} M) when more than 50 % displacement was found at 1 μM. Non-specific binding was determined in the presence of 10 μM AM630 (CHOK1hCB₂_bgal) or 10 μM SR141716A (CHOK1hCB₁_bgal). Incubation was terminated by rapid filtration through GF/C filters (Whatman International, Maidstone, UK), and followed by extensive washing using a Filtermate 96-well harvester (Perkin Elmer, Groningen, The Netherlands). Filter-bound radioactivity was determined by scintillation spectrometry using a 1450 Microbeta Wallac Trilux scintillation counter (Perkin Elmer).

Data analysis was performed by using the nonlinear regression curve fitting program GraphPad Prism 7.0 (GraphPad Software, Inc., San Diego, CA). From displacement assays, IC₅₀ values were obtained by non-linear regression analysis of the displacement curves. The obtained IC₅₀ values were converted into K_i values using the Cheng Prusoff equation [37] to determine the affinity of the ligands using a K_D value of [³H]CP55940 of 0.93 nM at CB₂R.

Supporting Information

Purity data of all compounds, additional synthetic procedures, general procedures for metabolism studies, determination of microsomal stability of **7a**, **23a** and **26a**, identification of metabolite structures of **7a**, **23a** and **26a**, determination of the logD_{7.4} value of **26a**, ¹H and ¹³C NMR spectra.

Acknowledgement

Financial support by the *Deutsche Forschungsgemeinschaft (DFG, collaborative*

research center 656 “Molecular Cardiovascular Imaging”) is gratefully acknowledged.

Conflict of interest

There is no conflict of interest.

References

- [1] Y. Gaoni, R. Mechoulam, Isolation, Structure, and Partial Synthesis of an Active Constituent of Hashish, *J. Am. Chem. Soc.* 86 (1964) 1646–1647. DOI: <http://dx.doi.org/10.1021/ja01062a046>.
- [2] E. Fride, R. Mechoulam, Pharmacological activity of the cannabinoid receptor agonist, anandamide, a brain constituent, *Eur. J. Pharmacol.* 231 (1993) 313–314. DOI: [http://dx.doi.org/10.1016/0014-2999\(93\)90468-W](http://dx.doi.org/10.1016/0014-2999(93)90468-W).
- [3] T. Sugiura, S. Kondo, A. Sukagawa, S. Nakane, A. Shinoda, K. Itoh, A. Yamashita, K. Waku, 2-Arachidonoylglycerol: a possible endogenous cannabinoid receptor ligand in brain, *Biochem. Biophys. Res. Commun.* 215 (1995) 89–97. DOI: <http://dx.doi.org/10.1006/bbrc.1995.2437>.
- [4] L.A. Matsuda, S.J. Lolait, M.J. Brownstein, A.C. Young, T.I. Bonner, Structure of a cannabinoid receptor and functional expression of the cloned cDNA, *Nature* 346 (1990) 561–564. DOI: <http://dx.doi.org/10.1038/346561a0>.
- [5] S. Munro, K.L. Thomas, M. Abu-Shaar, Molecular characterization of a peripheral receptor for cannabinoids, *Nature* 365 (1993) 61–65. DOI: <http://dx.doi.org/10.1038/365061a0>.
- [6] V. Di Marzo, The endocannabinoid system: its general strategy of action, tools for its pharmacological manipulation and potential therapeutic exploitation, *Pharmacol. Res.* 60 (2009) 77–84. DOI: <http://dx.doi.org/10.1016/j.phrs.2009.02.010>.
- [7] A.S. Heimann, I. Gomes, C.S. Dale, R.L. Pagano, A. Gupta, L.L. de Souza, A.D. Luchessi, L.M. Castro, R. Giorgi, V. Rioli, E.S. Ferro, L.A. Devi, Hemopressin is an inverse agonist of CB₁ cannabinoid receptors, *Proc. Natl. Acad. Sci. U. S. A.* 104 (2007) 20588–20593. DOI: <http://dx.doi.org/10.1073/pnas.0706980105>.

- [8] C. Turcotte, M.-R. Blanchet, M. Laviolette, N. Flamand, The CB₂ receptor and its role as a regulator of inflammation, *Cell. Mol. Life Sci.* 73 (2016) 4449–4470. DOI: <http://dx.doi.org/10.1007/s00018-016-2300-4>.
- [9] M. Roche, D.P. Finn, Brain CB₂ Receptors: Implications for Neuropsychiatric Disorders, *Pharmaceuticals* 3 (2010) 2517–2553. DOI: <http://dx.doi.org/10.3390/ph3082517>.
- [10] H.-C. Lu, K. Mackie, An Introduction to the Endogenous Cannabinoid System, *Biol. Psychiatry* 79 (2016) 516–525. DOI: <http://dx.doi.org/10.1016/j.biopsych.2015.07.028>.
- [11] A. Klegeris, C.J. Bissonnette, P.L. McGeer, Reduction of human monocytic cell neurotoxicity and cytokine secretion by ligands of the cannabinoid-type CB₂ receptor, *Br. J. Pharmacol.* 139 (2003) 775–786. DOI: <http://dx.doi.org/10.1038/sj.bjp.0705304>.
- [12] K. Maresz, E.J. Carrier, E.D. Ponomarev, C.J. Hillard, B.N. Dittel, Modulation of the cannabinoid CB₂ receptor in microglial cells in response to inflammatory stimuli, *J. Neurochem.* 95 (2005) 437–445. DOI: <http://dx.doi.org/10.1111/j.1471-4159.2005.03380.x>.
- [13] N.E. Buckley, K.L. McCoy, É. Mezey, T. Bonner, A. Zimmer, C.C. Felder, M. Glass, Immunomodulation by cannabinoids is absent in mice deficient for the cannabinoid CB₂ receptor, *Eur. J. Pharmacol.* 396 (2000) 141–149. DOI: [http://dx.doi.org/10.1016/S0014-2999\(00\)00211-9](http://dx.doi.org/10.1016/S0014-2999(00)00211-9).
- [14] J.W. Huffman, J. Liddle, S. Yu, M.M. Aung, M.E. Abood, J.L. Wiley, B.R. Martin, 3-(1',1'-Dimethylbutyl)-1-deoxy- Δ^8 -THC and related compounds: Synthesis of selective ligands for the CB₂ receptor, *Bioorg. Med. Chem.* 7 (1999) 2905–2914. DOI: [http://dx.doi.org/10.1016/S0968-0896\(99\)00219-9](http://dx.doi.org/10.1016/S0968-0896(99)00219-9).

- [15] M. Rinaldi-Carmona, F. Barth, J. Millan, J.M. Derocq, P. Casellas, C. Congy, D. Oustric, M. Sarran, M. Bouaboula, B. Calandra, M. Portier, D. Shire, J.C. Brelière, G.L. Le Fur, SR 144528, the first potent and selective antagonist of the CB₂ cannabinoid receptor, *J. Pharmacol. Exp. Ther.* 284 (1998) 644–650.
- [16] R.A. Ross, H.C. Brockie, L.A. Stevenson, V.L. Murphy, F. Templeton, A. Makriyannis, R.G. Pertwee, Agonist-inverse agonist characterization at CB₁ and CB₂ cannabinoid receptors of L759633, L759656, and AM630, *Br. J. Pharmacol.* 126 (1999) 665–672. DOI: <http://dx.doi.org/10.1038/sj.bjp.0702351>.
- [17] Y. Marchalant, P.W. Brownjohn, A. Bonnet, T. Kleffmann, J.C. Ashton, Validating Antibodies to the Cannabinoid CB₂ Receptor: Antibody Sensitivity Is Not Evidence of Antibody Specificity, *J. Histochem. Cytochem.* 62 (2014) 395–404. DOI: <http://dx.doi.org/10.1369/0022155414530995>.
- [18] M. Piel, I. Vernaleken, F. Rösch, Positron emission tomography in CNS drug discovery and drug monitoring, *J. Med. Chem.* 57 (2014) 9232–9258. DOI: <http://dx.doi.org/10.1021/jm5001858>.
- [19] R. Slavik, U. Grether, A. Müller Herde, L. Gobbi, J. Fingerle, C. Ullmer, S.D. Krämer, R. Schibli, L. Mu, S.M. Ametamey, Discovery of a high affinity and selective pyridine analog as a potential positron emission tomography imaging agent for cannabinoid type 2 receptor, *J. Med. Chem.* 58 (2015) 4266–4277. DOI: <http://dx.doi.org/10.1021/acs.jmedchem.5b00283>.
- [20] A. Haider, A. Muller Herde, R. Slavik, M. Weber, C. Mugnaini, A. Ligresti, R. Schibli, L. Mu, S. Mensah Ametamey, Synthesis and Biological Evaluation of Thiophene-Based Cannabinoid Receptor Type 2 Radiotracers for PET Imaging, *Front. Neurosci.* 10 (2016) 350. DOI: <http://dx.doi.org/10.3389/fnins.2016.00350>.
- [21] R. Slavik, A. Müller Herde, A. Haider, S.D. Krämer, M. Weber, R. Schibli, S.M. Ametamey, L. Mu, Discovery of a fluorinated 4-oxo-quinoline derivative as a

- potential positron emission tomography radiotracer for imaging cannabinoid receptor type 2, *J. Neurochem.* 138 (2016) 874–886. DOI: <http://dx.doi.org/10.1111/jnc.13716>.
- [22] R.-P. Moldovan, R. Teodoro, Y. Gao, W. Deuther-Conrad, M. Kranz, Y. Wang, H. Kuwabara, M. Nakano, H. Valentine, S. Fischer, M.G. Pomper, D.F. Wong, R.F. Dannals, P. Brust, A.G. Horti, Development of a High-Affinity PET Radioligand for Imaging Cannabinoid Subtype 2 Receptor, *J. Med. Chem.* 59 (2016) 7840–7855. DOI: <http://dx.doi.org/10.1021/acs.jmedchem.6b00554>.
- [23] L. Hortala, J. Arnaud, P. Roux, D. Oustric, L. Boulu, F. Oury-Donat, P. Avenet, T. Rooney, D. Alagille, O. Barret, G. Tamagnan, F. Barth, Synthesis and preliminary evaluation of a new fluorine-18 labelled triazine derivative for PET imaging of cannabinoid CB₂ receptor, *Bioorg. Med. Chem. Lett.* 24 (2014) 283–287. DOI: <http://dx.doi.org/10.1016/j.bmcl.2013.11.023>.
- [24] G. Saccomanni, G. Pascali, S.D. Carlo, D. Panetta, M. de Simone, S. Bertini, S. Burchielli, M. Digiaco, M. Macchia, C. Manera, P.A. Salvadori, Design, synthesis and preliminary evaluation of ¹⁸F-labelled 1,8-naphthyridin- and quinolin-2-one-3-carboxamide derivatives for PET imaging of CB₂ cannabinoid receptor, *Bioorg. Med. Chem. Lett.* 25 (2015) 2532–2535. DOI: <http://dx.doi.org/10.1016/j.bmcl.2015.04.055>.
- [25] M. Ahamed, D. van Veghel, C. Ullmer, K. van Laere, A. Verbruggen, G.M. Bormans, Synthesis, Biodistribution and In vitro Evaluation of Brain Permeable High Affinity Type 2 Cannabinoid Receptor Agonists [¹¹C]CMA2 and [¹⁸F]FMA3, *Front. Neurosci.* 10 (2016) 431. DOI: <http://dx.doi.org/10.3389/fnins.2016.00431>.
- [26] R. Teodoro, R.-P. Moldovan, C. Lueg, R. Günther, C.K. Donat, F.-A. Ludwig, S. Fischer, W. Deuther-Conrad, B. Wünsch, P. Brust, Radiofluorination and biological evaluation of N-aryl-oxadiazolyl-propionamides as potential

- radioligands for PET imaging of cannabinoid CB₂ receptors, *Org. Med. Chem. Lett.* 3 (2013) 11. DOI: <http://dx.doi.org/10.1186/2191-2858-3-11>.
- [27] C. Lueg, D. Schepmann, R. Günther, P. Brust, B. Wünsch, Development of fluorinated CB₂ receptor agonists for PET studies, *Bioorg. Med. Chem.* 21 (2013) 7481–7498. DOI: <http://dx.doi.org/10.1016/j.bmc.2013.09.040>.
- [28] T. Rühl, W. Deuther-Conrad, S. Fischer, R. Günther, L. Hennig, H. Krautscheid, P. Brust, Cannabinoid receptor type 2 (CB₂)-selective N-aryl-oxadiazolyl-propionamides: synthesis, radiolabelling, molecular modelling and biological evaluation, *Org. Med. Chem. Lett.* 2 (2012) 32. DOI: <http://dx.doi.org/10.1186/2191-2858-2-32>.
- [29] Y. Cheng, B.K. Albrecht, J. Brown, J.L. Buchanan, W.H. Buckner, E.F. DiMauro, R. Emkey, R.T. Freneau JR, J.-C. Harmange, B.J. Hoffman, L. Huang, M. Huang, J.H. Lee, F.-F. Lin, M.W. Martin, H.Q. Nguyen, V.F. Patel, S.A. Tomlinson, R.D. White, X. Xia, S.A. Hitchcock, Discovery and optimization of a novel series of N-arylamide oxadiazoles as potent, highly selective and orally bioavailable cannabinoid receptor 2 (CB₂) agonists, *J. Med. Chem.* 51 (2008) 5019–5034. DOI: <http://dx.doi.org/10.1021/jm800463f>.
- [30] M. Krasavin, A.V. Sosnov, R. Karapetian, I. Konstantinov, O. Soldatkina, E. Godovykh, F. Zubkov, R. Bai, E. Hamel, A.A. Gakh, Antiproliferative 4-(1,2,4-oxadiazol-5-yl)piperidine-1-carboxamides, a new tubulin inhibitor chemotype, *Bioorg. Med. Chem. Lett.* 24 (2014) 4477–4481. DOI: <http://dx.doi.org/10.1016/j.bmcl.2014.07.089>.
- [31] C. Lueg, F. Galla, B. Frehland, D. Schepmann, C.G. Daniliuc, W. Deuther-Conrad, P. Brust, B. Wünsch, Hydroxyalkylation with cyclic sulfates: synthesis of carbazole derived CB₂ ligands with increased polarity, *Arch. Pharm.* 347 (2014) 21–31. DOI: <http://dx.doi.org/10.1002/ardp.201300255>.

- [32] J. Henrottin, A. Zervosen, C. Lemaire, F. Sapunarcic, S. Laurent, B. van den Eynde, S. Goldman, A. Plenevaux, A. Luxen, N¹-Fluoroalkyltryptophan Analogues: Synthesis and in vitro Study as Potential Substrates for Indoleamine 2,3-Dioxygenase, *ACS Med. Chem. Lett.* 6 (2015) 260–265. DOI: <http://dx.doi.org/10.1021/ml500385d>.
- [33] M. Fujinaga, T. Yamasaki, J. Yui, A. Hatori, L. Xie, K. Kawamura, C. Asagawa, K. Kumata, Y. Yoshida, M. Ogawa, N. Nengaki, T. Fukumura, M.-R. Zhang, Synthesis and evaluation of novel radioligands for positron emission tomography imaging of metabotropic glutamate receptor subtype 1 (mGluR1) in rodent brain, *J. Med. Chem.* 55 (2012) 2342–2352. DOI: <http://dx.doi.org/10.1021/jm201590g>.
- [34] G. Bauer, G. Hägele, P. Sartori, Polyhalogenierte Ethane in der Kinnear-Perren-Reaktion, *Phosphorus Sulfur Relat. Elem.* 8 (2006) 95–98. DOI: <http://dx.doi.org/10.1080/03086648008078168>.
- [35] H. Ibrahim, F. Couderc, P. Perio, F. Collin, F. Nepveu, Behavior of *N*-oxide derivatives in atmospheric pressure ionization mass spectrometry, *Rapid communications in mass spectrometry RCM* 27 (2013) 621–628. DOI: <http://dx.doi.org/10.1002/rcm.6493>.
- [36] F. Galla, C. Bourgeois, K. Lehmkuhl, D. Schepmann, M. Soeberdt, T. Lotts, C. Abels, S. Ständer, B. Wünsch, Effects of polar κ receptor agonists designed for the periphery on ATP-induced Ca²⁺ release from keratinocytes, *Med. Chem. Commun.* 7 (2016) 317–326. DOI: <http://dx.doi.org/10.1039/C5MD00414D>.
- [37] C. Yung-Chi, W.H. Prusoff, Relationship between the inhibition constant (K_i) and the concentration of inhibitor which causes 50 per cent inhibition (I_{50}) of an enzymatic reaction, *Biochem. Pharmacol.* 22 (1973) 3099–3108. DOI: [http://dx.doi.org/10.1016/0006-2952\(73\)90196-2](http://dx.doi.org/10.1016/0006-2952(73)90196-2).

Graphical Abstract

